Optically Transparent Penning-trap electrodes for the ARTEMIS experiment

M. Voge1[1], G. Birkl[2], M. Ebrahimi[1], Z. Guo[1], N. Stallkamp[1] and W. Quint[1]

[1]GSI, Darmstadt, Germany; [2]Institut für Angewandte Physik, TU Darmstadt, Germany

We have conceived, built, and operated a cryogenic Penning trap with an electrically conducting yet optically transparent solid electrode [1,2]. The trap, dedicated to spectroscopy and imaging of confined particles under large solid angles in the ARTEMIS experiment [3,4] at HITRAP is of 'half-open' design, with one open endcap and one closed endcap that mainly consists of a glass window coated with a highly transparent conductive layer. This arrangement allows for trapping of externally or internally produced particles, yields flexible access for optical excitation and efficient light collection from the trapping region. At the same time, it is electrically closed and ensures long-term ion confinement under well-defined conditions. With its superior surface quality and its high and homogeneous optical transmission, the window electrode is an excellent replacement for partially transmissive electrodes that use holes, slits, metallic meshes and such.

Penning traps are valuable tools for precision spectroscopy of confined particles, largely owing to the multitude of available techniques for ion confinement and cooling. Confinement of internally or externally produced ions leads to a localisation of the species of interest in a small volume of space for long times. Cooling of these ions reduces shifts and transition line broadenings due to the Doppler effect, giving access to spectroscopy with high resolution and precision. To this end, a multitude of cooling techniques have been developed, which either require conducting surfaces close to the ions, good optical access, or both.

Our design is a so-called 'half-open' cylindrical Penning trap with the favourable electrical properties of a compensated open-endcap Penning trap, while at the same time surpassing its solid angle of optical access by more than an order of magnitude [3]. It features a window with transparent yet conductive coating, which has been characterized in a series of measurements, particularly with regard to its use in cryogenic Penning trap experiments.

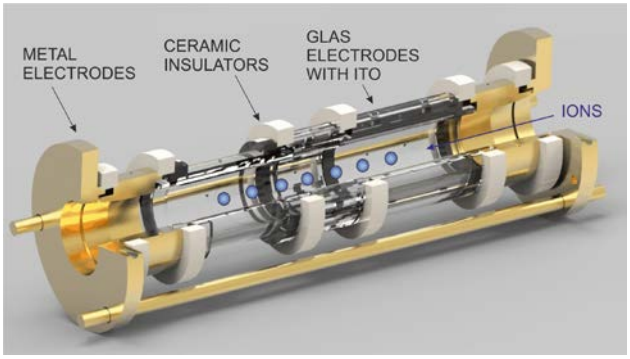

Figure 1: Artist's view of a possible further application of transparent electrodes with ITO coating on the inside, in a cylindrical Penning trap for spectroscopy of confined ions.

To the end of obtaining an optically transparent yet electrically closed electrode, a glass with an interior coating of ITO has been used. ITO is a doped n-type semiconductor with a bandgap of around 4 eV and is hence largely transparent in the visible part of the spectrum. It typically consists of about 75% indium (In), 17% oxygen (O2) and 8% tin (Sn) coated on a substrate. Several coating techniques are in use, including sputtering, spray coating and vapour deposition, all of which allow to fully coat or to produce 2D structures on the substrate surface, including bent substrates. ITO has a sheet resistance of around 80 Ohm/sq at a layer thickness of 125 nm. We have shown it to withstand cryogenic temperatures of down to 4 K, operation in a magnetic field of up to 7 Tesla, and resilience to impinging highly charged ions of keV kinetic energies per charge, while at the same time delivering a well-defined and stable electrostatic potential with a maximum surface roughness of few tens on nanometers, which is several orders of magnitude better than polished metal surfaces.

With this work we have introduced a novel realisation of Penning traps for precision spectroscopy, in which one endcap is made of a window with an electrically conductive yet optically transparent coating. This allows for a stable confinement of charged particles under well-defined conditions and efficient optical access to the confined particles under a large solid angle. This arrangement lends itself towards demanding applications such as optical precision spectroscopy of confined ions requiring efficient light collection. We have shown stable confinement of highly charged ions in such a trap and have studied the resilience and durability of an ITO-coated window used as an electrode in a cryogenic Penning trap environment.

References

[1] M. Wiesel, G. Birkl, M.S. Ebrahimi, A. Martin, W. Quint, N. Stallkamp, and M. Vogel, Rev. Sci. Inst. 88, 123101 (2017);

[2] L. Cockbill, Novel Penning trap design delivers optical access for precise spectroscopy, Scilight, DOI: 10.1063/1.5017839;

[3] D. von Lindenfels, M. Vogel, G. Birkl, W. Quint and M. Wiesel, Hyp. Int. 227, 197 (2014);

[4] D. von Lindenfels, M. Wiesel, W. Quint, D. Glazov, V.M. Shabaev, G. Birkl and M.Vogel, Phys. Rev. A 87, 023412 (2013)

Experiment beamline: HITRAP
Experiment collaboration: APPA-SPARC
Experiment proposal:
Accelerator infrastructure: SIS18, ESR
PSP codes:
Grants:
Strategic university co-operation with: Darmstadt

A scintillator-based ion detector for CRYRING@ESR*

C. Hahn[1,2,3], P. Pfäfflein[1,2,4], E. Menz[1,2], G. Weber[1,3] and Th. Stöhlker[1,2,3]

[1]HI Jena, Jena, Germany; [2]FSU, Jena, Germany; [3]GSI, Darmstadt, Germany; [4]DESY, Hamburg, Germany

The realization of the novel FAIR accelerator and storage ring complex achieved a major milestone with the commissioning of the CRYRING facility in late 2017. To fully exploit the multifaceted field of research thus made accessible, robust and reliable ion detectors are of fundamental importance [1]. These sensors will need to cope with MHz count rates of ions with energies ranging from sub-MeV/u to 15 MeV/u, and have to withstand the radiation damage imparted by the energetic ions. Given these restrictions, a detector system based on the YAP:Ce crystal scintillator provides an attractive approach, utilizing a material that is both comparatively affordable and endowed with a significant degree of radiation hardness [2].

A UHV-capable sensor design was devised and implemented as a collaborative effort of HI Jena, the University of Jena's Institute for Optics and Quantum Electronics, and the GSI Helmholtz Center. Figure 1 shows a cutaway view of the detector head: to accommodate the low end of the expected ion energy spectrum, the detector is essentially windowless, placing the scintillator material directly inside the vacuum. A light guide coupled to a fused silica window then channels the luminescence generated by the impinging ions to a photomultiplier tube (PMT) for conversion into an electrical signal. To facilitate the vacuum capability, this PMT – and all subsequent electronics – are kept on the atmospheric side of the window, and are installed only after the mandatory baking procedure is completed.

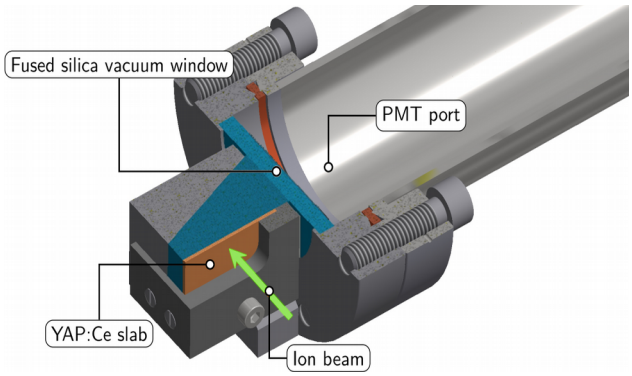

Figure 1: Schematic drawing of the detector head design. The ion beam hitting the scintillator induces light pulses which are registered by a photomultiplier tube attached to the atmospheric side of a UV-transparent vacuum window.

To gauge the assembly's sensitivity and long-term durability, a characterization measurement of this system, without the light guide prism, was conducted at the 3 MV tandem accelerator JULIA operated by the Institute of Solid State Physics at the University of Jena. Using hydrogen, oxygen and iodine ions at energies varying from 0.1 MeV/u to 2.4 MeV/u, the evolution of the PMT output signal was traced through increasing fluences of ion deposition inside the scintillator material, as illustrated by Figure 2. A marked decrease of the pulse height was found with proliferating damage: eventually, the output signal amplitude falls below the level of random noise pulses emitted by the PMT, at which point "true" events, i.e. pulses originating from incident ions, can no longer be reliably discerned by a simple pulse height threshold. This establishes a critical fluence, usually on the order of 10^{13} cm^{-2}, upon which the scintillator material has to be replaced. The exact magnitude of this fluence depends largely on the mass of the impinging ions; their kinetic energy plays only a minor role. On the other hand, the accumulating substrate damage does not appear to lead to an increase of the output pulse length past the initial value of about 50 ns, ensuring a uniform rate capability even after prolonged ion irradiation [3].

Building on the results of this successful proof-of-concept measurement, the final detector setup will be installed at CRYRING in early 2018.

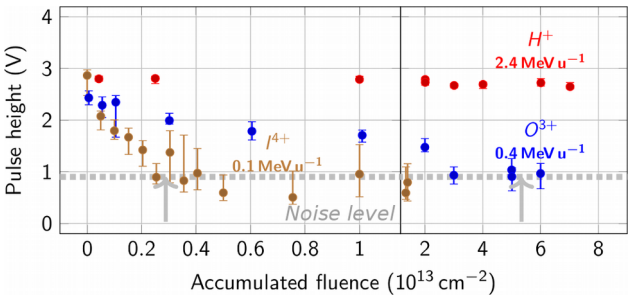

Figure 2: The average observed peak height for different ion species, at increasing accumulated fluences. Once the peak height reaches about 1 V, pulses originating from impinging ions can no longer be easily distinguished from random noise.

References

[1] M. Lestinsky et al., European Physics Journal Special Topics 225 (2016) 797
[2] M. Tokman et al., Physica Scripta 2001 (2001) 406
[3] P. Pfäfflein, "Entwicklung und Aufbau eines Teilchendetektors für erste Experimente am Ionenspeicherring CRYRING", Masterarbeit, Friedrich-Schiller-Universität Jena (2017)

Experiment beamline: CRYRING
Experiment collaboration: SPARC
Experiment proposal: none
Accelerator infrastructure: CRYRING
PSP codes: none
Grants: none
Strategic university co-operation with: none

*This report is also part of the HI Jena Scientific Report 2017.

 DOI:10.15120/GR-2018-1

Atomic computations of hyperfine coupling constants *

R. Beerwerth[1,2] and S. Fritzsche[1,2]

[1]Helmholtz Institute Jena, Germany; [2]Theoretisch-Physikalisches Institut, Friedrich Schiller University Jena, Germany

Precise spectroscopic measurements of hyperfine structures and isotope shifts allow to extract information about the nucleus under investigation, such as mean squared charge radii, deformation, nuclear spin and nuclear moments [1]. With the help of isotope separator online facilities that allow the production of atomic beams for large chains of isotopes one can probe these quantities for many short-lived nuclei. Recent advances [2] now open the perspective to extend these studies also into the region of superheavy elements, such as nobelium and in the near future lawrencium in order to probe possible regions of increased stability.

The hyperfine coupling constants A and B relate the nuclear magnetic dipole μ and electric quadrupole moments Q to the magnetic field and electric field gradients generated by the electrons at the site of the nucleus, respectively. Both of these quantities can be determined experimentally by measuring the same transition in different isotopes, if the nuclear moments are known for one of these isotopes. Alternatively, both hyperfine coupling constants can be computed from atomic many-body theory such as the multi-configuration Dirac-Fock (MCDF) method [3]. For iron, the only stable odd mass isotope ^{57}Fe with nuclear spin ½ does not have a quadrupole interaction, and consequently no quadrupole moment was known so far. In order to extract the nuclear quadrupole moment of ^{53}Fe, we performed extensive MCDF calculations of the hyperfine constants for the $3d^6 4s^2\ ^5D_4$ ground level and the $4s4p\ ^5F_5$ excited level [4]. Since the nuclear dipole moment and its coupling constants are well known, the A values for both levels were used as a benchmark to test the computations. Our result for B was subsequently used to extract Q.

Several independent model calculations were performed to provide an estimate of the theoretical uncertainty. Each model computation was performed in a systematically enlarged configuration space, which was generated by virtual single and double excitations of the valence electrons. Especially the magnetic dipole interaction of the ground level was strongly influenced by core effects. To account for these effects, single excitations from the core orbitals had to be incorporated into the generation of the atomic basis and lead to an agreement between experiment and theory at the 10% level.

Our computed results are shown in Fig. 1, where every circle marks the result of one model calculation of the hyperfine coupling constants for the ground or excited level. The results clearly show that the A-factor for the ground level deviates significantly from experiment when no core effects are considered. This effect does not happen for the excited level, since here the main contribution to the hyperfine interaction comes from the uncoupled *s*-electron and hence core effects are much less significant. The *B*-factors for both levels scatter much less, which, together with the good agreement of the *A*-factors with the experimental values, leads to the conclusion that an uncertainty of 15%, shown as coloured bar, for the computed values seems reasonable. The black lines denote the experimentally determined coupling constants with additional input from nuclear theory, whose error bars are not shown here.

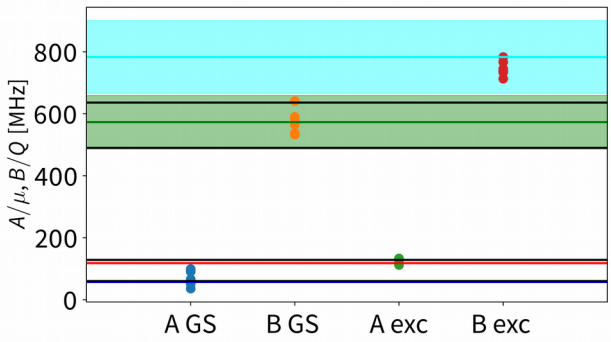

Figure 1: Computed hyperfine coupling constants A and B for the $^5D_4$ ground (GS) and $^5F_5$ excited Level of neutral ^{53}Fe from different model computations (circles). The black lines denote experimental values, the coloured lines the adopted values from our computations and the coloured bars the computational uncertainty.

In summary, atomic computations can provide valuable input in interpreting experimental data and in this case helped to extract nuclear properties. The combination of independent model calculations and systematically enlarged configuration spaces can provide estimates of theoretical uncertainties.

References

[1] M. Block, Hyperfine Interact. 238 (2017), 40
[2] M. Laatiaoui et al., Nature 538 (2016), 495-498
[3] P. Jönsson et al., Comput. Phys. Commun. 177 (2007), 597622
[4] A. J. Miller et al., Phys. Rev. C 96 (2017), 054314

* Also part of the Annual Report 2017, Helmholtz Institute Jena

Elastic scattering of twisted light by hydrogenlike ions*

A. A. Peshkov[1], A. V. Volotka[1] , A. Surzhykov[2,3], and S. Fritzsche[1,4]

[1]Helmholtz-Institut Jena, Germany; [2]Physikalisch-Technische Bundesanstalt, Braunschweig, Germany; [3]Technische Universität Braunschweig, Germany; [4]Friedrich-Schiller-Universität Jena, Germany

The elastic scattering of photons by the bound electrons of atoms or ions, commonly known as Rayleigh scattering, has been intensively explored over the past decades. From a theoretical viewpoint, the Rayleigh scattering has attracted much interest as one of the simplest second-order quantum electrodynamical (QED) process. In the past, a large number of experimental and theoretical studies have been performed in order to understand how the electronic structure of atoms affects the polarization of the Rayleigh-scattered photons. In particular, the linear polarization of the elastically scattered light has been measured directly by Blumenhagen et al. at the PETRA III synchrotron at DESY [1]. This experiment was performed for a gold target with a highly linearly polarized incident plane-wave radiation. Until the present, however, very little has been known about the Rayleigh scattering of twisted (or vortex) light beams. When compared to plane-wave radiation, such twisted photons have a helical wave front and carry a well-defined projection of the orbital angular momentum upon their propagation direction. In addition, the transverse intensity profile of the twisted beams exhibits a ringlike pattern with a dark spot (vortex) at the center. In experiments, twisted (Bessel) beams can nowadays be readily produced by means of spatial light modulators or axicons.

In the present work, we analyze theoretically the behavior of the polarization Stokes parameters of scattered photons for the elastic scattering of twisted Bessel light. Here we restrict ourselves to the nonresonant Rayleigh scattering of light by hydrogenlike ions in their ground state, and especially by hydrogenlike carbon. We consider and derive the Stokes parameters within the framework of second-order perturbation theory and the density-matrix approach. Three different possible experimental scenarios are considered here for the scattering of the incident Bessel beam at a single atom, a mesoscopic (atoms in a trap), or a macroscopic (foil) atomic target, and which are all assumed to be centered on the beam axis. We show that the linear and circular polarization of scattered light depends generally on the helicity and the opening angle of Bessel beams, leading to Stokes parameters that differ quite significantly from the scattering of incident plane-wave photons. Moreover, results of our calculations indicate that the polarization of the scattered photons is very sensitive to the projection of the total angular momentum (TAM) of twisted light for single atoms and mesoscopic atomic targets of a few tens of nm in size, while it remains unaffected by the TAM in the case of a larger macroscopic target. In particular, Figure 1 illustrates the first Stokes parameter, which characterizes the degree of linear polarization of outgoing photons, as a function of the scattering angle for mesoscopic target. As seen from this figure, the outgoing photons are completely linearly polarized at the scattering angle 90 degrees for incoming plane waves. However, the scattering of a Bessel beam by mesoscopic target with the width of 10 nm, for example, leads to a significant decrease of the polarization at this angle, depending on the TAM projection of twisted light.

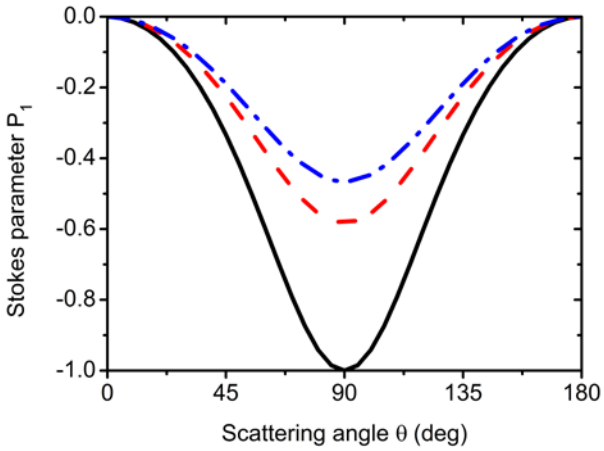

Figure 1: Stokes parameter of Rayleigh scattered light on hydrogenlike carbon ions in their ground state as a function of the emission angle. Results for incident plane waves (black solid lines) are compared with those for Bessel beams with TAM +1 (red dashed lines) and -1 (blue dash-dotted lines), respectively. Relativistic calculations were performed for mesoscopic atomic target of size 10 nm. Results are shown for the helicity +1, opening angle 30 degrees, and photon energy 100 eV of a Bessel beam.

Although our study was restricted to the scattering by hydrogenlike ions in their ground 1s state, similar polarization properties can also be observed in the scattering of twisted light by electrons in other s shells. In view of this, Rayleigh scattering may serve as an accurate technique for measuring the properties of twisted beams in a wide range of photon energies, and in particular at rather high energies.

References

[1] K.-H. Blumenhagen S. Fritzsche, T. Gassner, A. Gumberidze, R. Märtin, N. Schell, D. Seipt, U. Spillmann, A. Surzhykov, S. Trotsenko, G. Weber, V. A. Yerokhin, and T. Stöhlker, New J. Phys. 18 (2016) 103034.

[2] A. A. Peshkov A. V. Volotka, A. Surzhykov, and S. Fritzsche, Phys. Rev. A 97 (2018) 023802.

*Also part of the Annual Report 2017, Helmholtz Institute Jena.

 DOI:10.15120/GR-2018-1

The spin-polarised electron target PEGASUS

D. Schury[1,2],M. Lestinsky[1],A. Kalinin[1],S. Schippers[2],S. Hagmann[1],C. Kozhuharov[1],T. Stöhlker[1,3,4]

[1]GSI, Darmstadt, Germany; [2]JLU Gießen, Gießen, Germany; [3]HI Jena, Jena, Germany; [4]FSU Jena, Jena, Germany

A source for spin-polarised electrons for experiments on (highly charged) ions at storage rings has been built. Its performance is presently being characterized.

Chirality is a prominent characteristic of the molecular building blocks of life. It refers to the mirror symmetry of the spatial structure of a molecule. The influence of the differences in the positions of the nuclei in the molecule on chemical reactions has been widely studied in chemistry. In contrast, effects of molecular chirality on the electronic structure and dynamics have received much less attention. The ELCH collaboration (Electrodynamics of chiral systems) was formed with partners from different hessian universities to conduct research on chirality and related symmetries covering a wide range of topics from the molecular domain to strong field processes in highly charged ions. Within this collaboration, a source for spin-polarised electrons has been built at GSI [1].

In this source (see Figure 1), the spin-polarised electrons are extracted from a bulk GaAs semiconductor photocathode by polarised laser radiation [2]. The vacuum setup is divided into three sections. In the first section, the cathode is heat-cleaned and prepared into a state of negative electron-affinity [3]. By an alternating inlet of molecular oxygen and caesium into the preparation chamber, approximately one monolayer of oxidized caesium is produced on the cathode, which dramatically enhances its quantum efficiency. After preparation, the cathode is transferred to the adjacent section where it is irradiated by a near-infrared solid-state laser to generate a beam of spin-polarized electrons. In the same section, the electrons are accelerated to an energy of up to 10 keV. After acceleration, the beam is deflected by a 90° electrostatic bender to separate the electron beam from the laser beam and to achieve a transversal polarization with respect to the beam propagation direction. The third section is used for the analysis of the electron-beam properties and for providing a connection to experiments. Currently, we can measure intensity, lateral profile, energy distribution, and the degree of the transversal polarisation of the electron-beam. For the determination of the latter quantity a mini-MOTT detector is attached. Already our first beams exhibited a polarization degree of about 25%. The compact setup with a footprint of only 2 m^2 is mobile and can be easily used at different storage rings, as well as at other facilities.

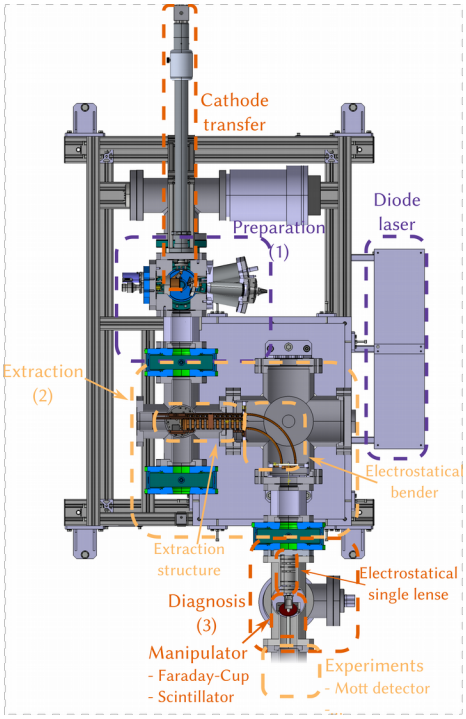

Figure 1: Schematic overview of the setup.

A number of technical improvements are foreseen: In the future, strained superlattice cathodes[4] will deliver polarization degrees of up to 90 %. The cathode handling shall be improved to keep more than one sample prepared simultaneously. Additionally, atomic hydrogen is planned for improved in-vacuum reconditioning of the cathode surface.

The only element manipulating the electron spin so far is the electrostatic bender which turns the polarisation from longitudinal to transversal. By adding two adjacent Wien-filters it will become possible to deliberately select the spin-orientation according to the experimental requirements.

References

[1] D. Schury, Construction and characterization of a spin-polarized electron source for future experiments with chiral molecules, PhD Thesis, Justus-Liebig University Gießen, 2017.
[2] D. Pierce, F. Meier and P. Zürcher, Appl. Phys. Lett. (26), 1975
[3] H. Sonnenberg, Appl. Phys. Lett. (14), 1969
[4] T. Nishitani, et al., J. Appl. Phys. (97), 2005

Experiment beamline: none
Experiment collaboration: APPA-SPARC
Experiment proposal: none
Accelerator infrastructure: none
PSP codes: none
Grants: H2020 ERC-2015-CoG/LOEWE-ELCH 05E12CD2
Strategic university co-operation with: Gießen

A third amplifier stage in the pulse system for laser cooling of relativistic ion beams at SIS100

D. Kiefer[1] and Th. Walther[1]

[1]Institute of Applied Physics, TU-Darmstadt, Darmstadt, Germany

Laser cooling has been demonstrated in the ESR and is planned for SIS100 as well as for HESR. With the aim of achieving white light cooling [1] of relativistic heavy ion beams, a pulsed laser system with adjustable repetition rate and spectral width is under development.

The principle of the laser system has been presented elsewhere [2] and the Fourier limited character of the laser pulses has been investigated [3]. A first test of the second harmonic generation [4] has been reported. In brief, the system consists of an external cavity diode laser (ECDL), whose radiation at 1028 nm is amplified, followed by a fast electro-optic modulator stage producing the laser pulses between 70 and 740 ps. Finally, two fiber based amplifier stages are used to increase the available average power. In the final system there will be nonlinear frequency conversion to the 4th harmonic. However, the results discussed here were achieved at 1028 nm. In order to achieve pulse energies high enough for cooling of even the heaviest elements [5], we installed an additional third amplifier stage to the pulse laser system. This amplifier stage consists of a backward pumped air-clad fiber. The 80 cm long fiber rod has a core diameter of 85 microns, resulting in a mode field area over 40 times larger than that of the second amplifier stage. This helps to avoid nonlinear effects as well as intensity induced damage. The pump cladding diameter is 260 microns and the rod is temperature stabilized by a water chiller. The fiber allows polarization-maintaining single-mode operation. Due to the currently available maximum cw pump power of 27 W at 976 nm, the amplification is limited. An even further increase of the pulse energies should be possible with a stronger pump laser source.

For laser cooling with short laser pulses, the pulse energy has to be adjusted to each different ion species, preferably with the repetition rate scalable to the ion velocity and the number of buckets. Therefore, the laser system is developed to provide flexibility in both energy and repetition rate. Table 1 shows the achieved pulse energies and average powers dependent on repetition rate and pulse duration. The pulse energies increase with pulse duration. The average power is independent of repetition rate, indicating that there is no saturation at our pump levels. Thus, more pump power will significantly increase the output power and pulse energies providing a fairly straightforward way to reach even higher energies.

Table 1: Pulse energies in J and average power in W observed after three ampli er stages

Rep.Rate	Pulse Duration		
	250 ps	500 ps	735 ps
1 MHz	11 J, 11 W	13 J, 13 W	15 J, 15 W
5 MHz	2.2 J, 11 W	2.6 J, 13 W	3 J, 15 W

The sinc^2-shaped frequency spectrum of the output measured with a slowly scanning Fabry-Pérot interferometer (FPI, Free Spectral Range (FSR) 10 GHz) with a FWHM of 1.86 GHz is shown in figure 1. The inset shows the corresponding rectangular timing signal. The time bandwidth product equals 0.93 suggesting Fourier transform limited pulses.

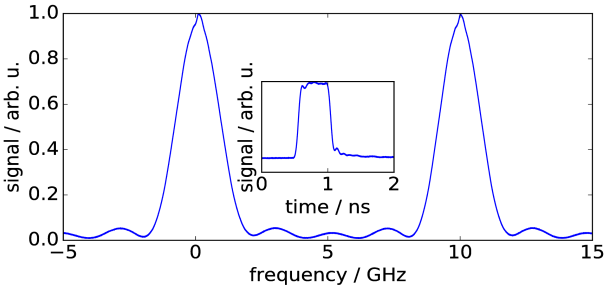

Figure 1: Spectrum and corresponding temporal shape (inset) of a rectangular pulse of 500 ps duration after the third amplifier stage. The spectrum was observed with a slowly scanning FPI (FSR 10 GHz). These results are independent of the repetition rate.

References

[1] R. Calabrese, V. Guidi, P. Lenisa et al.,"White-light laser cooling of ions in a storage ring" Hyperfine Interact 99: 259, 1996

[2] T. Beck and Th. Walther, "A flexible pulsed ps/ns laser system for ion beam cooling at ESR/SIS100", GSI Scientific Report 2014

[3] D. Kiefer, T. Beck and Th. Walther, "Flexible Picosecond Master Oscillator Fiber Amplifier System for Ion Beam Laser Cooling at ESR/SIS100", GSI Scientific Report 2015

[4] D. Kiefer, S. Klammes, B. Rein and Th. Walther, "Recent Work on the Darmstadt laser systems for laser cooling of relativistic ion beams at SIS100", GSI Scientific Report 2016

[5] L. Eidam, O. Boine-Frankenheim, D. Winters, "Cooling rates and intensity limitations for laser-cooled ions at relativistic energies", Nuclear Instruments and Methods in Physics Research Section A: Accelerators, Spectrometers, Detectors and Associated Equipment, Volume 887, Pages 102-113, 2018

Experiment beamline: ESR
Experiment collaboration: APPA-SPARC
Experiment proposal: E136
Accelerator infrastructure: ESR / SIS100 / HESR
PSP codes: none
Grants: funded by BMBF, grant number 05P15RDFA1.

 DOI:10.15120/GR-2018-1

Auger cascade calculations in krypton supporting pump–probe experiments*

S. O. Stock[1,2], R. Beerwerth[1,2], and S. Fritzsche[1,2]

[1]Helmholtz Institute Jena, Germany; [2]Theoretisch-Physikalisches Institut, Friedrich Schiller University Jena, Germany

Recent advances in experimental techniques such as ultrafast time-resolved spectroscopy and modern UV and X-ray sources have enabled detailed studies of ionization processes. In order to interpret the results of these experiments, large-scale atomic structure computations are an important tool. Here, we report our theoretical results in support of a recent experimental study of the ionization dynamics in inner-shell excited krypton [1].

The experiment employs a pump–probe scheme and for the first time combines absorption spectroscopy and photoion spectroscopy to give a detailed picture of the ionization dynamics. The pump pulse, an attosecond XUV beam centered around 90 eV, excites the $3d^{-1}np$ resonances in neutral krypton while an intense few-cycle near-infrared (NIR) pulse acts as probe by (doubly) ionizing different groups of Kr^+ ions to Kr^{3+}. Through variation of the NIR intensity, different groups of levels can be "reached" by the probe pulse which allows a detailed view into the ionization dynamics (see Ref. [1] for details). By varying the delay between XUV and NIR pulse, one gains access to the lifetimes of the levels which are ionized by the NIR pulse.

In order to support the experiment, we performed extensive multiconfiguration Dirac–Fock calculations using the GRASP [2] and RATIP [3] packages. After excitation by the XUV pulse, the $3d^{-1}np$ excited atoms decay predominantly by a two-step Auger cascade. We model this decay cascade by considering all possible normal Auger decays as well as shake processes of the *np* valence electron, in an approach similar to our recent theoretical studies [4,5]. All calculations are performed at a fine-structure level in order to obtain a comprehensive view of the autoionization paths.

An overview of the Auger cascade following the resonant $3d^{-1}np$ excitation is given in Fig. 1. In the first step of the cascade, the inner-shell excited krypton atoms decay predominantly via spectator Auger decays to the $4p^{-2}np$, $4s^{-1}4p^{-1}np$, $4p^{-3}4dnp$, and $4s^{-2}np$ levels, while participator processes can be neglected. In the second step of the cascade, the $4s^{-1}4p^{-1}np/4p^{-3}4dnp$ levels autoionize further to the ground configuration of Kr^{2+} while the $4s^{-2}np$ levels autoionize to the Kr^{2+} $4s^{-1}4p^{-1}$ and $4p^{-3}4d$ configurations.

Even though only a few of the autoionizing Kr^+ levels (marked with the numbers 1–12 in Fig. 1) are predominantly populated during the first step of the cascade, their lifetimes range from a few femtoseconds to several hundred femtoseconds. Since the experiment cannot access the decay curves of individual levels, but instead rather large groups of levels within an energy range, we calculate *effective* lifetimes, as a weighted average of the individual lifetimes, for different level groups. While the $4s^{-2}np$ levels have an effective lifetime of only 6 fs, the $4s^{-1}4p^{-1}np/4p^{-3}4dnp$ levels decay considerably slower, with an effective lifetime of 49 fs. This difference in effective lifetimes is consistent with the experimental findings where a higher NIR intensity leads to a longer apparent lifetime, since lower-lying levels are being addressed by the probe pulse.

In conclusion, comprehensive theoretical studies of Auger cascades are important to support new kinds of experiments with modern UV and X-ray sources.

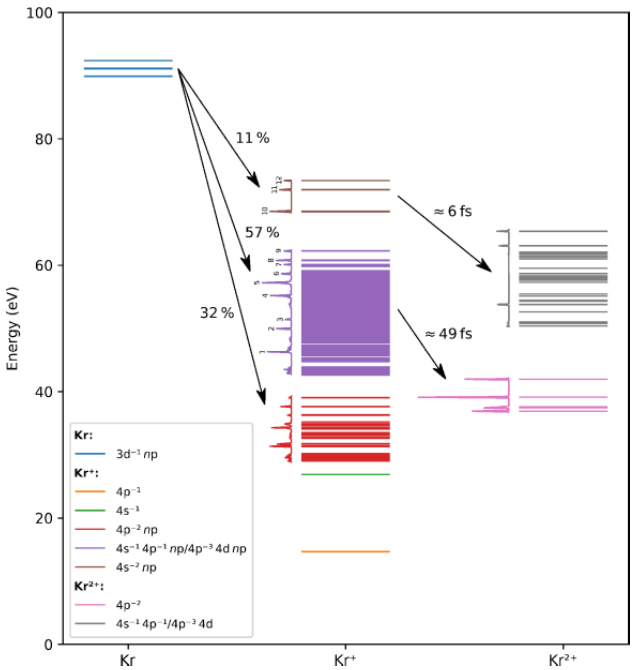

Figure 1: Diagram of the levels involved in the two-step Auger cascade after resonant $3d^{-1}np$ excitation of Kr. The spectra to the left of each group of levels show the relative population of the respective levels. Energies are given relative to the ground level of neutral krypton. The $4s^{-1}4p^{-1}np$ and $4p^{-3}4dnp$ configurations of Kr^+ as well as the $4s^{-1}4p^{-1}$ and $4p^{-3}4d$ configurations of Kr^{2+} are mixing heavily and are therefore not clearly distinguishable.

References

[1] K. Hütten et al., Nat. Commun. 9 (2018), 719
[2] P. Jönsson et al., Comput. Phys. Commun. 177 (2007), 597–622
[3] S. Fritzsche, Comput. Phys. Commun. 183 (2012), 1525–1559
[4] S. Schippers et al., Phys. Rev. A 94 (2016), 41401
[5] S. Stock, R. Beerwerth, and S. Fritzsche, Phys. Rev. A 95 (2017), 53407

*Also part of the Annual Report 2017, Helmholtz Institute Jena

Elliptical dichroism in two-photon atomic ionization

J. Hofbrucker[1,2], A. V. Volotka[1], S. Fritzsche[1,2]

[1] Helmholtz Institute Jena [2]Friedrich-Schiller Universität Jena

Dichroic behavior is usually associated with an interaction of polarized atomic or chiral molecular target and circularly polarized light. Since the observations of asymmetries in above-threshold ionization of nobel gases by elliptically polarized light [1], it became apparent that a dichroic behavior is not a unique characteristic of a chiral target, but can also arise from a non-linear light-matter interaction. In contrast to circular dichroism, it arises from the interference of the dominant ionization channels. It is solely the interference between the different ionization channels which carries the information about the sign of the elliptical polarization. Since the elliptical dichroism is system specific, it gives us an opportunity to study many-electron effects as well as fundamentals of non-linear light-matter interaction.

In our recent work, we studied the intriguing phenomenon of elliptical dichroism in two-photon ionization of a *K*-shell electron of neutral atoms by elliptically polarized light [2, 3]. It was found that a strong effect can be found at threshold energies for two-photon ionization of light elements. However, for inner-shell ionization, high energy photons are required, but the polarization control at current free-electron laser facilities is scarce. In cooperation with our experimental colleagues from the European XFEL project, we decided to find an experimental system for verification of inner-shell elliptical dichroism within the limits of current technologies (proposal 20174073 at FERMI). Out of rare gas atoms, electrons from the krypton *3p* shell were chosen as the most convenient showcase to detect a strong two-photon ionization elliptical dichroism (see Figure 1). Since the cross section for a direct two-photon ionization of Kr *3p* is relatively low and two-photon absorption requires comparably long acquisition times for obtaining statistically valid spectra, we proposed to study the elliptical dichroism in the vicinity of the Kr *3p-3d* resonance in order to facilitate the feasibility of the experiment. The photoelectron spectra will be measured for five photon energies, covering the dynamical energy dependence of the elliptical dichroism, including measurements of both strong and zero dichroism.The proposed experiment of two-photon ionization of Kr will be the first confirmation of elliptical dichroism in inner-shell ionization and it will give us the opportunity to accurately extract atomic parameters relevant for the ionization process.

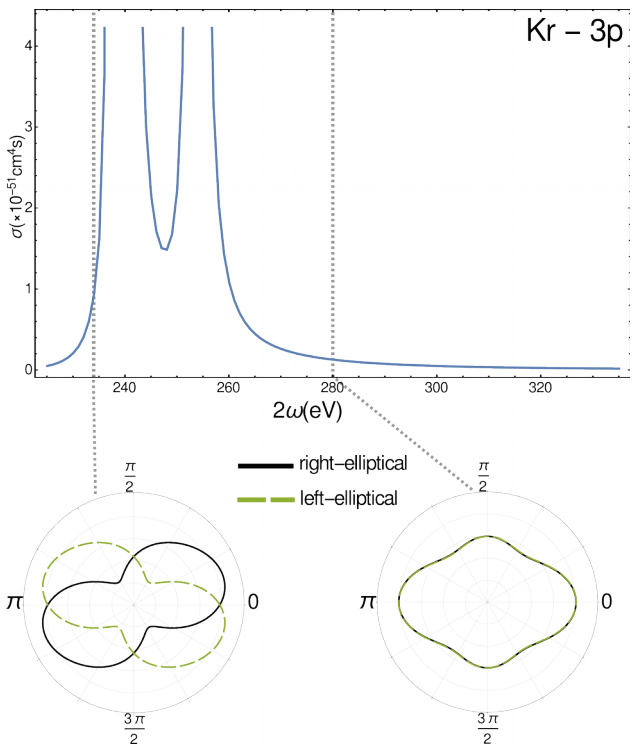

Figure 1: (Upper): Total two-photon cross section in the range of the Kr *3p-3d* resonance as a function of two-photon energy (energy transferred to the initially bound electron). (Lower): Electron distributions in the plane perpendicular to the photon propagation (dipole plane) are shown for two energy points. These distributions represent the maximal and minimal elliptical dichroism for the two-photon ionization of Kr *3p*. From the figures, it is apparent that the dichroism is highly sensitive to the photon (or photoelectron) energy. It is worth noting that the resonance itself only plays a secondary role in the process.

References

[1] M. Bashkansky, P. H. Bucksbaum, and D. W. Schumacher, Phys. Rev. Lett. 60, 2458 (1988).

[2] J. Hofbrucker, A. V. Volotka, and S. Fritzsche, Phys. Rev. A 94, 063412 (2016).

[3] J. Hofbrucker, A. V. Volotka, and S. Fritzsche, Phys. Rev. A 96, 013409 (2017).

Also part of the Annual Report 2017, Helmholtz Institute Jena

 DOI:10.15120/GR-2018-1

Towards a quantum standard for high voltage measurements

K. König[1], J. Krämer[1], C. Geppert[2], P. Imgram[1], B. Maaß[1], J. Meisner[3], E. W. Otten[4], S. Passon[3], T. Ratajczyk[1], J. Ullmann[1] and W. Nörtershäuser[1]

[1]Institut für Kernphysik, TU Darmstadt, Germany, [2]Institut für Kernchemie, JGU Mainz, Germany, [3]Physikalisch Technische Bundesanstalt, Germany, [4]Institut für Physik, JGU Mainz, Germany

Many experiments, e.g. at the ESR or at KATRIN rely on accurate high voltage measurements. These are usually carried out with high voltage dividers which are limited to an accuracy of up to 1 ppm [1] due to an intricate, step-wise calibration tracing back to low-voltage Josephson standards [2]. The susceptibility of the resistors to thermal changes and aging effects is the main source of systematic uncertainties and prohibits a long-term stability [3].

On the contrary, a stable quantum standard for high voltage measurements could be defined with collinear laser spectroscopy: If an atom or ion beam is superposed collinearly by a laser beam, the laboratory-frame laser frequency ν_L will be Doppler-shifted according to

$$\nu_L = \nu_0 \, \gamma \, (1 \pm \beta) \qquad (1)$$

for co-/counter-propagating beams in the rest frame of the moving particles. For an electrostatically accelerated ion with the charge q and mass m, the velocity β is defined by the potential difference U since

$$qU = mc^2(\gamma - 1)\,. \qquad (2)$$

Solving Eq. 1 and 2 for the acceleration potential, the applied voltage is linked to the measurement of a laser frequency only by fundamental constants

$$U = \frac{mc^2}{2q} \frac{(\nu_L - \nu_0)^2}{\nu_L \nu_0}. \qquad (3)$$

Hence, for ions with well-known mass and transition frequency ν_0 the applied voltage can be determined, if the laser frequency in the laboratory frame is identified. This can be realized e.g., with a laser scan while observing the fluorescence light emitted by the excited ions.

Earlier attempts with this technique were limited by the uncertainty of the optical frequency measurement [4] or the uncertainty of the real starting potential of the ions in the ion source [5]. In the ALIVE (Accurate Laser Involved Voltage Evaluation) experiment a two-stage laser interaction for a pump and probe approach is combined with a highly accurate frequency determination with a frequency comb [6] to overcome these limitations.

In this first stage of the experiment we used calcium ions produced in a surface ion source and compared the achieved results with a Julie Research Laboratory HVA100 and the PT20 high voltage divider from the Physikalisch-Technische Bundesanstalt (PTB) which both have a 5 ppm relative uncertainty.

We have performed a measurement series with voltages between -5 kV and -19 kV. The deviation of the laser spectroscopic measurement from the simultaneous measurement with the voltage dividers is shown in Fig. 1. The black error bars indicate the statistical uncertainty whereas the green error bars represent a systematic uncertainty due to a possible misalignment of the post acceleration stage which was identified as the main source of systematic uncertainty and always shifts the measured voltage to smaller values. Within the uncertainty of the voltage dividers of 5 ppm our results are in good agreement.

In the next phase of the experiment we will use indium ions produced with very low transverse emittance in a liquid metal ion source. This will allow smaller apertures leading to a better overlap and hence a higher accuracy by better ion beam collimation. Furthermore, the transition will be very narrow, allowing higher precision in the determination of the resonance position. With these improvements we think that we will be able to reach an accuracy better than 1 ppm.

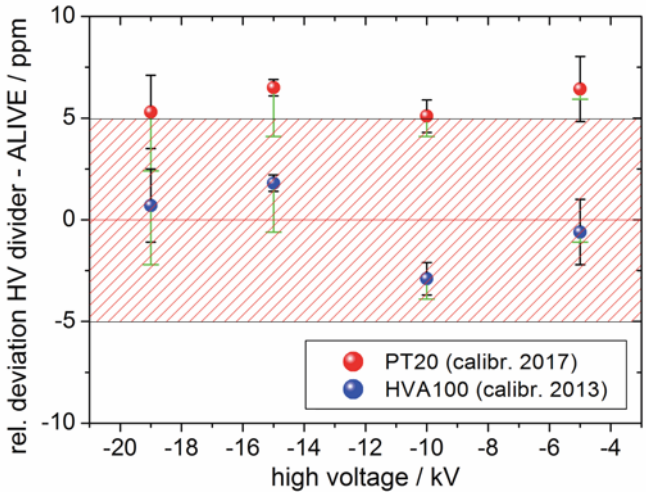

Figure 1: Results of the high voltage measurement [7]. The relative deviation of the laser spectroscopic from the electronic measurement is shown as a function of the voltage for the two high voltage dividers. The shaded area marks the uncertainty of the voltage dividers used in this experiment. For more details see text.

References

[1] T. Thümmler, et. al., New J. Phys., 11 (2009) 103007
[2] B. Josephson, Phys. Lett., 1 (1962) 251
[3] K. Kim, et. al, IEEE Trans. Instr. Meas.,52 (2007) 469
[4] O. Poulsen, E.Riis, Metrologia, 25 (1988) 147
[5] S. Götte, et.al., Rev. Sci. Instr., 75 (2004) 1039
[6] T. Udem, et. al., Nature, 416 (2002) 233
[7] J. Krämer, K. König, et. al., Metrologia (2018) https://doi.org/10.1088/1681-7575/aaabe0

Experiment beamline: CRYRING / ESR
Experiment collaboration: APPA-SPARC
Experiment proposal: none
Accelerator infrastructure: ESR / CRYRING
PSP codes: none
Grants: HIC for FAIR, DFG INST 163/392-1 FUGG, HGS-HIRE
Strategic university co-operation with: Darmstadt

Towards a solution of the hyperfine puzzle of strong-field bound-state QED

J. Ullmann[1,2], S. Schmidt[1,3] and W. Nörtershäuser[1]
L. Skripnikov[4], A. Volotka[4,5], and V. Shabaev[4]

[1] TU Darmstadt, Institut für Kernphysik, Darmstadt, Germany; [2]Westfälische Wilhelms-Universität Münster, Institut für Kernphysik, Münster, Germany; [3]Johannes Gutenberg-Universität Mainz, Institut für Physik, Mainz Germany; [4]St. Petersburg State University, Department of Physics, St. Petersburg, Russia; [5]Helmholtz-Institut Jena, Jena, Germany

The first high-precision measurement of the so-called specific difference $\Delta' E = \Delta E_{2s} - \xi \Delta E_{1s}$ of the hyperfine structure splitting in hydrogen-like $^{209}Bi^{82+}$ and lithium-like $^{209}Bi^{80+}$ was reported in [1] and analysed as a test of bound-state quantum electrodynamics (BS-QED) in strong fields, where a pertubative description of QED is no longer possible. It was found that the experimental value deviates by more than 7σ from the theoretical prediction, giving rise to the so-called hyperfine puzzle of BS-QED. The result has triggered many discussions in the community, as it has the potential to challenge BS-QED.

Here, we summarize the efforts to provide a solution of this hyperfine puzzle. As already pointed out in [1], there are three possible explanations for the observed discrepancy: (1) new physical effects not considered in current QED calculations, (2) a wrong nuclear magnetic moment of bismuth, as this experimentally determined value enters linearly into the specific difference, or (3) an unexpected deficiency in the specific difference. In the following we will concentrate on points (2) and (3), which both have to be clarified before (1) can be considered.

To examine the nuclear magnetic moment of ^{209}Bi, we have performed NMR measurements in collaboration with the group of Prof. M. Vogel (TU Darmstadt) on $Bi(NO_3)_3$ dissolved in concentrated and diluted nitric acid to study effects of the chemical environment. In parallel, state-of-the-art calculations of the diamagnetic correction and the chemical shift were carried out. The NMR measurements were performed at an 8.4-T magnet using the same temperature stabilized double resonance probe for ^{209}Bi NMR and ^{1}H NMR calibration with tetramethylsilane (TMS). The observed effects of temperature and acidity in the $Bi(NO_3)_3$ solution could hardly be explained by model calculations, due to the unknown quantity of water molecules involved in the hydration of the Bi^{3+} ions. A much cleaner system concerning the chemical shift, yet experimentally harder to handle, turned out to be the hexafluoridobismuthate(V) (BiF_6^-) anion, which has a high spatial symmetry. The sample was prepared in an elaborate process by the fluoride specialist group of Prof. F. Kraus (University of Marburg). During the NMR measurement of this sample, the typical septet structure in the spectrum was observed, which uniquely assures the chemical environment. Moreover, the temperature dependency was insignificant in this case. The knowledge of the chemical environment in this sample strongly reduced the uncertainty of the chemical shift correction, which previously has been the dominant uncertainty. The specific difference based on this new nuclear magnetic moment agrees within uncertainties with the experimental value in [1]. This indicates an explanation for a large part of the deviation [2]. Clear evidence requires a correction-free measurement, e.g., at the ARTEMIS trap experiment.

Possibility (3) from above can be examined by extending the measurement of the specific difference to the isotopic sequence in bismuth, in particular ^{208}Bi and ^{207}Bi. The results will give new insights into nuclear structure theory, specially our understanding of the magnetic distribution inside the nucleus (Bohr-Weisskopf effect). The proposed studies are foreseen to be carried out at the experimental storage ring at GSI.

As a prerequisite towards laser spectroscopy of H-like and Li-like ^{208}Bi, a more precise value of its nuclear magnetic moment is mandatory. Moreover, a new value will lead to better predictions of the transition wavelength under investigation, which is important for spectroscopy experiments of this kind. Therefore, the hyperfine structure (hfs) splitting (hyperfine *A* and *B* factors) of this isotope were measured at the collinear laser spectroscopy experiment (COLLAPS) at ISOLDE, CERN, with improved accuracy. By combining these results with theoretical calculations of the hfs anomaly, we have provided a new value for the nuclear magnetic moment of ^{208}Bi based on the magnetic moment of ^{209}Bi that was determined from the ESR experiments reported in [1] under the assumption that QED is correct [3]. In addition, we have obtained theoretical predictions of the ground-state hyperfine transition energies, which are 5600(4) meV and 878.1(5) meV for H-like and Li-like ^{208}Bi, respectively [3].

The results present an important step towards a first measurement of the specific difference using a radioactive isotope. Hereby, a major challenge will be the reduced fluorescence rate due to the lower beam intensity in the storage ring. For H-like ^{208}Bi the production rate will be sufficient to follow an optical detection scheme. In contrast, for lithium-like ^{208}Bi and for ^{207}Bi ions, more dedicated detection methods are necessary, which are currently being developed (see [4]).

References

[1] J. Ullmann et al., Nature Comm. 8, 15484 (2017)
[2] L. Skripnikov et al., PRL **120**, 093001 (2018)
[3] S. Schmidt et al., Phys. Lett. B **779**, 324 (2018)
[4] M. Lestinsky, et al., Eur. Phys. J. **225** 797 (2016)

Experiment beamline: ESR
Experiment collaboration: APPA-SPARC
Experiment proposal: E128
Grants: BMBF 05P15RDFAA; HIC for FAIR; SPbSU-DFG (Grants No. 11.65.41.2017 and No. STO 346/5-1); DFG VO 1707/1-3
Strategic university co-operation with: Darmstadt

 DOI:10.15120/GR-2018-1

Highly Charged Ions at the HILITE Penning trap experiment

N. Stallkamp[1,2,3], S. Ringleb[3], M. Kiffer[3], S. Kumar[4], T. Morgenroth[1,3], G. Paulus[2,3], W. Quint[1,5], Th. Stöhlker[1,2,3] and M. Vogel[1]

[1]GSI, Darmstadt, Germany; [2]Helmholtz-Institut Jena; [3]Friedrich Schiller Universität Jena; [4]Inter-University Accelerator Centre, New Delhi, [5]Ruprecht Karls-Universität Heidelberg

High-sensitivity measurements of reaction educts and products of laser-particle interactions benefit from a preparation of the target ensemble in a well-defined way. Therefore, we have conceived, designed and built the HILITE Penning trap experiment. It employs ion-cloud formation techniques as well as destructive and non-destructive techniques to analyse the trap content for all species and charge states individually and simultaneously [1]. This facilitates reconstruction of non-linear interactions of stored particle species with high-energy and/or high-intensity lasers.

In order to be independent from external ion sources and to be able to perform experiments at different laser facilities, a dedicated ion source is needed, which fulfils the key requirement of the complete setup, namely to be easily transportable. For that purpose, a compact electron beam ion source (EBIS) together with a dedicated control and readout system (see Fig.1) has been implemented and brought into operation [2].

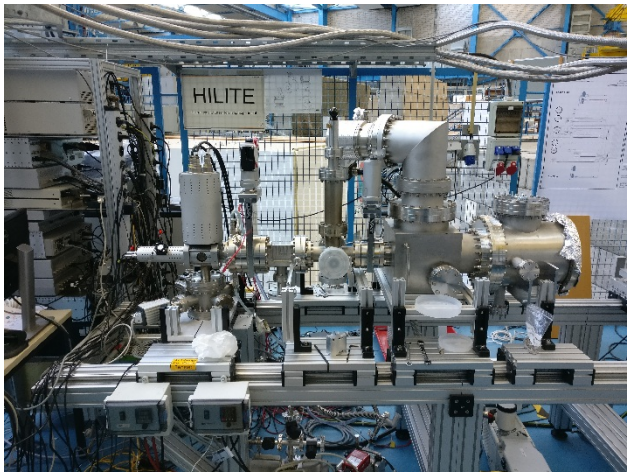

Figure 1: Ion source setup (EBIS, left) with attached diagnostic chamber (right).

We have measured the voltage switching times for ion deceleration and ion capture to verify the performance when slowing down ions extracted from the EBIS for subsequent storage in the HILITE trap. After capture, the ions will initially have kinetic energies of the order of 200 eV. For fast and efficient ion slowing, we have developed a novel implementation of 'active ion slowing', where the ion-signal induced in one trap electrode segment is used for negative feedback. Consequently, the ions experience a repulsive force when approaching the electrode and an attractive when leaving it. Obviously, feeding the slowing signal back to the pick-up electrode causes a strong overlap between ion signal and the slowing signal itself. To overcome this issue, we have implemented a balanced Wheatstone bridge consisting of four capacitors, one of which is the trap electrode itself. The voltages applied to both branches are subtracted from each other. In consequence, the difference is the pure ion signal, as this is only induced in one of the branches. The circuit diagram and the manufactured electronics board used in our trap is shown in figure 2. First tests show, that both branches can be balanced out well.

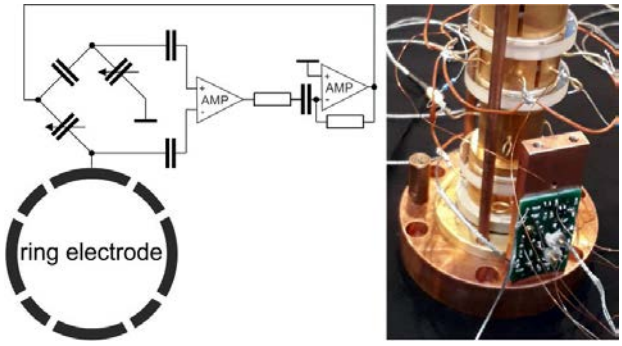

Figure 2: Feedback ion-cooling circuit and photo of the electronics board attached to the trap.

Following this active feedback slowing, we will apply cooling techniques to further cool the ion ensemble down to the environmental temperature of about 4K. This will be done by the well-known 'resistive cooling' technique, where the ions lose energy by dissipating power to a cryogenic resonance resistance. Such cooling facilitates the application of various ion manipulation techniques for control over ion density, position and the overall composition of the target ion ensemble confined in the trap.

*Also part of the annual report 2017, Helmholtz-Institut Jena

References

[1] S. Ringleb, M. Vogel, S. Kumar, W. Quint, G. Paulus, Th. Stöhlker, Journal of Physics Conference Series 635 (2015) 092124

[2] T. Morgenroth, Master thesis, Uni Jena 2017

Experiment beamline: none
Experiment collaboration: APPA-SPARC
Experiment proposal: none
Accelerator infrastructure: none
PSP codes: none
Grants: none

First online applications of the LASPEC DAQ system

S. Kaufmann[1], K. König[1], I. Metzler[1], F. Sommer[1] and W. Nörtershäuser[1]

[1]TU Darmstadt, Darmstadt, Germany;

Bunched-beam collinear laser spectroscopy (CLS) has become very popular in the recent years, due to the impressive background suppression in the order of 10^4 which results from the temporal control of the ions. This allows to perform experiments with exotic isotopes that are produced at rates of only a few 100 ions/s and will also be used in the LASPEC experiment at FAIR.

In order to match these experimental conditions, a new time resolved data acquisition (DAQ) system was developed during the last years at the LASPEC collinear ion beamline TRIGA-LASER [1]. It is called TILDA (**TRI**GA **L**ASER **D**ata **A**cquisition) and its real-time operations are realised by two FPGAs located in a PXI-crate. The flexibility of the FPGAs ensures that the system can be adapted to various experimental conditions required for collinear laser spectroscopy since a variety of detection techniques can be applied. Thanks to the high-level programming languages python and LabVIEW in combination with a sophisticated layer architecture, new developers can adapt TILDA to their needs in short time.

One of the first tests for TILDA was the offline commissioning campaign of the radio frequency cooler and buncher (RFQCB) at the MATS-LASPEC-prototype TRIGA-SPEC [1,2]. The next step in development was then its first passive online usage at the COLLAPS experiment at ISOLDE-CERN in parallel to a well-established data acquisition that lacks photon-timing capabilities. The benefits of TILDA's time resolution became quickly obvious during this measurement campaign, since it provides important information about the proper operation of the RFQCB that cannot be easily obtained by other means. In 2017, TILDA became the main data acquisition system for COLLAPS and was successfully used during two online measurement campaigns. In the upper part of Figure 1, a typical spectrum of this campaign is shown for ^{61}Ni.

Furthermore, TILDA is now implemented also at the COALA beamline (**Co**llinear **A**pparatus for **L**aser Spectroscopy and **A**pplied Physics) in Darmstadt, which serves now as the German development platform for LASPEC, while the TRIGA-laser beamline is operated at Argonne (USA) within FAIR phase 0. Here, TILDA has been adapted to implement also the possibility of fast laser switching using acousto-optical modulators (AOM). The advantage of laser-beam switching for example to avoid hyperfine pumping of the small components in a spectrum was demonstrated at TRIUMF previously and will also be of advantage at LASPEC.

At GSI it is planned to implement TILDA as the DAQ system for laser spectroscopy experiments at CRYRING.

References

[1] S. Kaufmann, et al., Journal of Physics: Conference Series 599-1-012033 (2015)

[2] Ch. Gorges, S. Kaufmann, Hyperfine Interactions **238**, 26 (2017)

[3] I. Metzler, Bachelor Thesis, TU Darmstadt (2017)

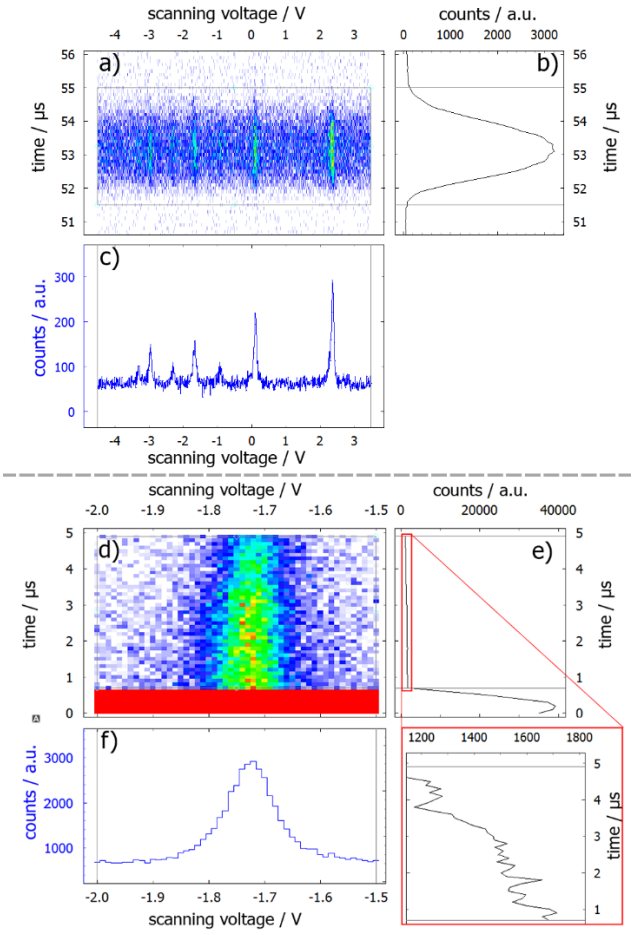

Figure 1: The application of TILDA's timing resolution with a pulsed ion beam of ^{61}Ni (a-c) and a "pulsed" laser beam (d-f) (switched off by an AOM at 0.7 µs) to visualize the versatility of the time-resolved DAQ. Graphs a,d: color coded fluorescence count rate as a function of the Doppler-tuning voltage (*x*-axis) and the time of flight (*y*-axis) relative to a timing trigger (in (a) the time after the extraction of the ions from ISCOOL, in (d) 0.7 µs before the pump laser is turned off). Graphs b,e: temporal projection of the number of counts within the marked region of interest (ROI) onto the time axis from which information on the bunch structure (c) or the excitation profile along the ion beam (e) can be extracted. Graphs e,f: resonance lineshape as a function of the Doppler-tuning voltage. For more details see [2,3].

Experiment beamline: none
Experiment collaboration: NUSTAR-LASPEC
Experiment proposal: none
Accelerator infrastructure: none
Grants: BMBF contract 05P15RDFN
Strategic university co-operation with: Darmstadt

 DOI:10.15120/GR-2018-1

Cooling time constant of ions stored in Penning traps

A. Henkel[1,2,3], F. Herfurth[1], R. Pinnau[2] and T.-K. Strempel[3,]

[1]GSI, Darmstadt, Germany; [2]Technische Universität Kaiserslautern, Germany; [3]University of Applied Sciences, Darmstadt, Germany

The HITRAP (Highly Charged Ions Trap) facility at GSI allows to investigate slow highly charged ions up to U^{92+}. The most important part of the facility is the Penning trap, which allows the trapping of ions.

A microscopic simulation of the ion cloud is only possible to a limited extent [1]. For this reason, based on [2] we derive two new models, the *global* and *local cooling model*. The global cooling model describes the cooling constant of the center-of-mass motion. While the local cooling model describes the cooling constant of the internal motion.

The cooling model

In contrast to [2] the starting point of both cooling models is the differential equation of the resonant circuit for the voltage

$$\frac{d^2u(t)}{dt^2}+\frac{R}{L}\frac{du(t)}{dt}+\frac{1}{LC}u(t)=\frac{R}{LC}\left(i(t)+\frac{L}{R}\frac{di(t)}{dt}\right) \qquad (1)$$

with resistor R, inductor L, capacitor C and current *i(t)*. The electrical power

$$P(t)=\frac{energy}{time}=\frac{dE_{kin}(t)}{dt}=-u(t)i(t) \qquad (2)$$

can be used to link the kinetic energy $E_{kin}(t)$ of the system with the resonant circuit equation (1). The minus sign in (2) is due to the fact that the energy in the resonant circuit is dissipated and will not be returned to the system.

The global cooling constant

For the global current $i_G(t)$ we choose the approach

$$i_G(t)=\frac{1}{\sqrt{12}}q\kappa\sqrt{N}\sqrt{\frac{2E_{kin}^G(t)}{m}}\cos(\omega_{res}t)$$

with the kinetic center-of-mass energy E_{kin}^G, mass *m*, number of particles *N*, charge *q*, resonance frequency ω_{res} and a constant of proportionality κ. Now (1) and (2) can be solved numerically. The results are shown in Figure 1.

An analytical solution of the system (1) and (2) can not be given. But if we assume that the kinetic energy is almost not changed compared to the current over an oscillation period, the system can be reduced to a driven harmonic oscillator whose solution is known. Assuming the center-of-mass is in resonance with the resonant circuit, we get the global cooling time constant

$$\tau_G=\frac{12m}{q^2N\kappa^2R_{res}} \qquad (3)$$

with the resonance resistance R_{res}.

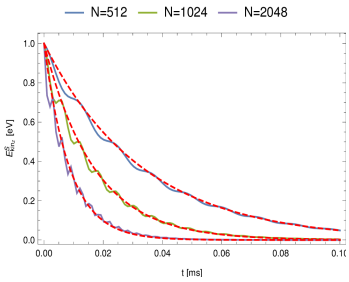

Figure 1: The red dashed lines are the solutions of the global cooling model and the others are the solutions of the microscopic model.

The local cooling constant

For the local current $i_L(t)$ we choose the approach

$$i_L(t)=q\kappa\frac{\sqrt{N}}{N}\sqrt{\frac{k_BT(t)}{m}}\cos(\omega_{res}t)$$

with the BOLTZMANN constant k_B, the temparatur T und use the relationship between mean kinetic energy and temperature.

Analogous to the global model, if we assume that the temperature hardly changes compared to the current over an oscillation period, the system of differential equations can be solved.

We get the local cooling time constant

$$\tau_L=\frac{3mN}{q^2\kappa^2R_{res}}. \qquad (4)$$

If we compare both cooling time constants (3) and (4), it is noticeable that with τ_G the numer of particles N appears in the denominator and by τ_L in the numerator. If we increase the number of particles, more particles contribute to the current during the center-of-mass motion, which results in rapid global cooling. Instead, the local cooling slows down. This is because the velocities are cancelled out.

References

[1] Henkel, A. et al. GSI Scientific Report 146, 2015.

[2] VOGEL, M., et al. Resistive and sympathetic cooling of highly-charged-ion clouds in a Penning trap. *Physical Review A*, 2014, 90. Jg., Nr. 4, S. 043412.

Precision spectroscopy using a maXs microcalorimeter

M. O. Herdrich[1,2,3], G. Weber[1,2], A. Fleischmann[4], D. Hengstler[4], and Th. Stöhlker[1,2,3]

[1]HI Jena; [2]IOQ, FSU Jena, [3]GSI, Darmstadt, [4]KIP, RKU Heidelberg

Introduction

A new generation of cryogenic microcalorimeters for usage as high precision X-ray spectrometers is currently under development for the SPARC collaboration. The maXs-30 of the maXs (microcalorimeter array for X-ray spectroscopy) detector design developed by the group of Prof. Enss at KIP, Heidelberg features 64 pixels and a theoretical energy resolution of 5 eV FWHM at 6 keV photon energy with an accessible energy range from several 100 eV up to 100 keV [1]. A fast signal rise time (≈100 ns) enables coincidence measurements with time resolutions in the order of 10 ns. Combined with a high linearity [2] and a good long-term stability, the maXs detector system is well suited for high precision measurements at storage rings such as the ESR or CRYRING at GSI/FAIR. First experiments have already been conducted using a prototype detector in the beginning of 2016 and preliminary results were obtained using a new signal processing algorithm based on finite response filters. The new method is more stable and due to much a faster execution time allows for an online analysis of the detector signals.

Preliminary Results

The experiment was conducted at the ESR using U^{89+} ions with a beam energy of 80 MeV/u in collision with a N_2 gas target. A maXs-30 detector was positioned at 90° with respect to the beam axis, with a ≈10 cm air gap to the interaction chamber. Preliminary results (see fig. 1) show that an energy resolution of approx. 80 eV is achieved throughout the whole energy range of the detector using the newly designed finite response filter for data analysis. This is only 10 eV worse compared to the commonly used optimal filter algorithm [3] which is too computational expensive for online analysis of the measured data. Insufficient temperature control of the detector and noise induced by the ESR might explain the divergence from the theoretical optimal resolution. Nevertheless, a comparison with results from experiments with He-like Uranium conducted by X. Ma et. al in 2000 [4] shows that the achieved energy resolution already surpasses the one of standard semiconductor-based X-ray detectors be a factor of 5. Further improvements can be expected with a better temperature correction. The rather small ratio between the intra-shell transition Δn=0 and the Balmer lines compared to theory is explainable by the absorption of the photons in the air gap and two Beryllium windows which act like a high pass filter for X-rays. A detailed simulation of the collision system is planned to determine the spectral lines as well as to separate radiation stemming from capture and excitation processes.

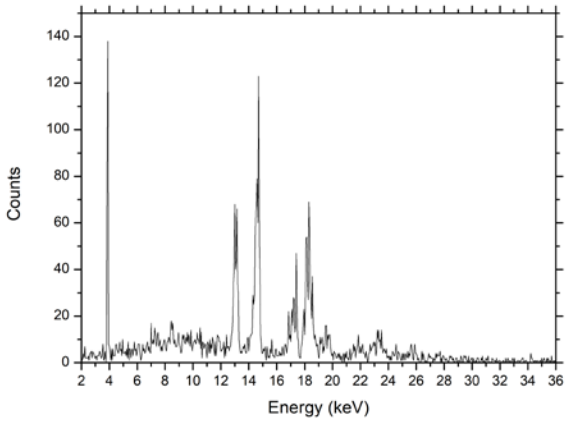

Figure 1: Preliminary results showing an X-ray spectrum recorded at the ESR for U^{89+} collisions with N_2 at 80 MeV/u. Visible are the inner shell transition Δn=0 in the L-shell ($1s_2\ 2p_{3/2} \rightarrow 1s_2\ 2s_{1/2}$) of the projectile as well as several Balmer ($n > 2 \rightarrow L$) and Paschen ($n > 3 \rightarrow M$) transitions. Radiation resulting from both capture and excitation of the projectile can be seen.

Conclusion and Outlook

The analysis of first experimental data recorded by the maXs-30 detector shows that results generated with the new algorithm are comparable to the results of the optimal filter. Planned improvements include a recently updated version of the maXs-30 detector, which contains a temperature sensitive pixel. Every global temperature change of the detectors shifts its operating point and thereby changes the baseline of the detector signals. By reading out the baseline of the temperature sensitive pixel for every read-out cycle, a correlation between energy and working point can be found. A simple bilinear correction is applied to compensate temperature induced shifts of the read-out energy. First tests show, that this method is highly effective in resolving artificial multipeak structures arising from an unstable operation point.

References

[1] D. Hengstler et al., Phys. Scr. T166, 2015
[2] C. Enss et al., J. Low Temp. Phys., Vol. 121, 2000
[3] A. Fleischmann, Dissertation, RKU Heidelberg, 2003
[4] X. Ma et al., Phys. Rev. A, Vol. 64, 2001

Experiment beamline: ESR

Experiment collaboration: APPA-SPARC
Accelerator infrastructure: ESR
Grants: This work is supported by the European Union and the federal state of Thuringia via Thüringer Aufbaubank within the ESF program (2015 FGR 0094).
Strategic university co-operation with: Friedrich-Schiller-University Jena

This report is also part of the HIJ Annual Report 2017

 DOI:10.15120/GR-2018-1

The Transverse Electron Target for CRYRING@ESR

C. Brandau[1,2], A. Borovik, Jr.[1], B.M. Döhring[1], B. Ebinger[1], M. Lestinsky[2], T. Molkentin[1], A. Müller[1], S. Schippers[1] for the SPARC working group 'Electron Targets'

[1]Justus-Liebig-Universität Gießen, Germany; [2]GSI, Darmstadt, Germany

As outlined in the CRYRING@ESR Physics Book of the SPARC collaboration and the CRYRING Instrumentation TDR [1, 2] it is planned to install a ribbon-shaped free-electron target in the experimental section YR09 of CRYRING@ESR [3]. The target will be mainly used for atomic electron-ion collision studies and is optimized for operation in the storage ring environment of CRYRING. The target can be fully retracted from the storage ring behind a gate valve. The target will be concurrently installed in the experimental section YR09 with the gas-jet target allowing for an optimal use of beam time. The electron beam interacts with the ion beam under a collision angle of 90° with a free sight field to the interaction zone for photon spectroscopy (Fig. 1).

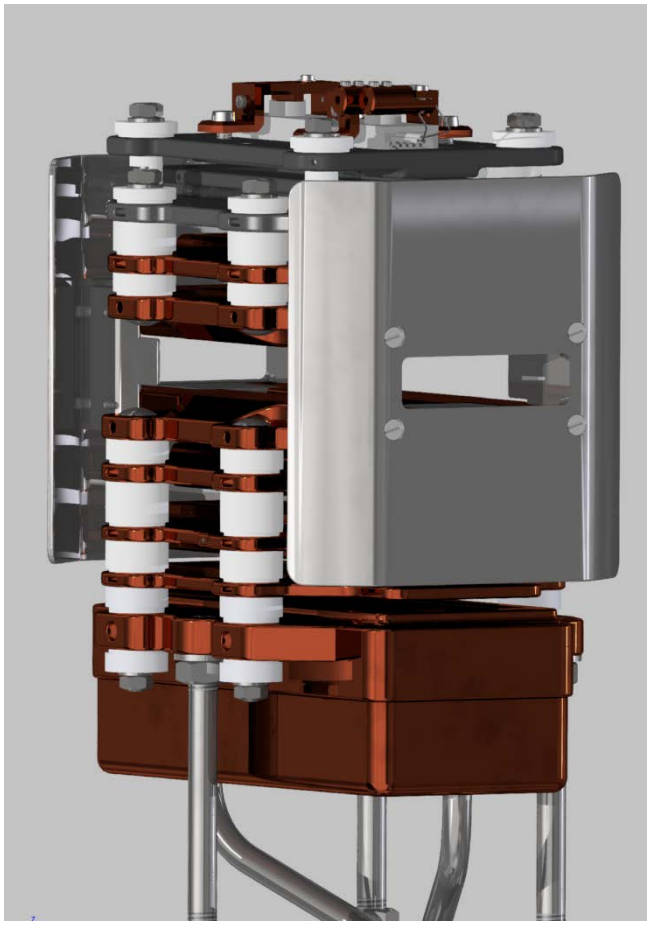

Figure 1: CAD model of the electron gun for the CRYRING@ESR transverse electron target. The electron beam is directed from top to bottom. Behind the interaction region, the beam is decelerated and dumped in the collector. The ion beam passes the gun through the shielding apertures at the front and at the back. The geometrical overlap of electron and ion beam can be controlled and quantified by moving the gun in the horizontal direction. The interaction volume is open from both sides providing a large solid angle for photon spectroscopy.

The electron gun features a high-energy mode up to 12.5 keV electron energy, and a high-density mode with electron densities surpassing $n_e = 1 \cdot 10^9$ cm^{-3}. Further details of the target and the envisaged set-up in the CRYRING experimental section are given in [4, 5].

During the last year, further options were added to the gun and the design of the gun-electrodes was finalized (Fig. 1). It is now foreseen to pulse the voltage of the first anode that controls the electron emission from the cathode. This feature allows the electron beam to be swiftly switched off during phases with no ion beam in the ring, thus substantially reducing the heat-load on the collector and, hence, the gas-load to the ring-vacuum. In addition, it will be investigated whether the switching can also be used for timing purposes. Four electrodes at the side of the interaction zone enable the shaping of the potential, e.g., to flatten the space charge potential of the electron beam for a more precise energy definition of the electrons and higher experimental resolution as well as to avoid trapping of slow ions from the residual gas. Like the anode, the clearing/shaping electrodes' voltages can be pulsed to swiftly switch between different modes (e.g., flat potential, trapping, non-trapping).

The electrodes and other parts of the gun are presently being manufactured. Vacuum recipients, pumps, the main manipulator and a first set of power supplies have been ordered and are partially already delivered. We expect to assemble the target and to perform first offline tests by the end of 2018. Depending on additional funding, the target will be available in CRYRING@ESR in 2021.

References

[1] M. Lestinsky et al., Eur. Phys. J Spec. Top. **225** (2016), 797.
[2] Z. Andelkovic et al., Technical Design Report: Experimental Instrumentation of CRYRING@ESR, 2015, http://www.fair-center.eu/en/en/for-users/experiments/appa/documents.html.
[3] M. Lestinsky et al., Phys. Scr. T**166** (2015), 014075.
[4] C. Brandau et al., GSI Scientific Report 2015, p. 143.
[5] C. Brandau et al., GSI Scientific Report 2016, p. 240.

Experiment beamline: CRYRING
Experiment collaboration: APPA-SPARC
Experiment proposal: none
Accelerator infrastructure: CRYRING
PSP codes: 1.3.1.5.9
Grants: BMBF contract No. 05P15RGFAA and HIC for FAIR
Strategic university co-operation with: Gießen

Status of a new laser ablation ion beam source for LASPEC

T. Ratajczyk[1], V. Varentsov[2,3] and W. Nörtershäuser[1]

[1]Institut für Kernphysik, TU Darmstadt, Germany, [2]Facility for Antiproton and Ion Research in Europe (FAIR GmbH), Darmstadt, Germany, [3]Institute for Theoretical and Experimental Physics, Moscow, Russia

Continuous and pulsed ion beams having low emittances are required for many high precision laser spectroscopy experiments. A high quality and compact source of various stable ions is for example needed for the LASPEC project [1]. A multi-purpose collinear beamline has been installed at TU Darmstadt [2] and will serve as the German development platform for LASPEC. An ion source that can provide high quality beams in a wide range of stable isotopes is an ideal tool to be used for further improvement of the system performance, for precision laser spectroscopy and to test the whole setup to ensure efficient operation during online measurements of the radioactive isotopes at FAIR. The ion source might also be used at CRYRING to provide additional ion species.

The laser ablation ion source of a new type that is under construction at TU Darmstadt is based on the proposal described in details in [3]. It combines the ion production by laser ablation in presence of helium gas, ion extraction via a supersonic gas jet into an RF-only ion funnel and then into original RF-buncher placed downstream in high vacuum conditions. The schematics of this ion source together with results of a gas dynamics simulation for the gas velocity flow field is shown in Figure 1.

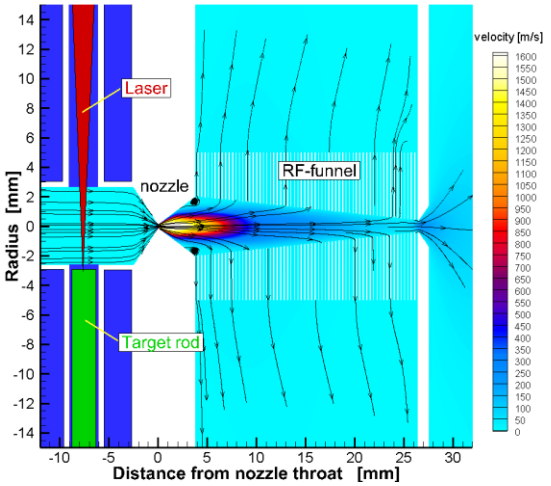

Figure 1. Schematics of the new laser ablation ion source together with the results of gas dynamics simulation of its operation. The Rf-buncher behind the RF-only funnel is not shown.

The CAD-rendering of the setup design is shown in Fig. 2. This ion source system has been manufactured, assembled (see Fig. 3) and first gas dynamic measurements were recently performed. These measurements are in a good agreement with full Navier-Stokes gas dynamics simulations (flow fields of gas temperatures, densities and velocity components), which have been used for detailed ion trajectory Monte Carlo simulations.

The main calculated parameters of the extracted ion beam (ablated from the aluminium target at He stagnation pressure of 200 mbar) are as follows: Beam energy - 92.6 eV, longitudinal energy spread (90% level) - 0.018 eV, beam radius (90% level) - 0.74 mm, transverse emittance - 16.3 π mm mrad, time of bunching - 1 ms, extracted bunch width - 5 µs, longitudinal emittance (90% level) - 0.09 eV µs.

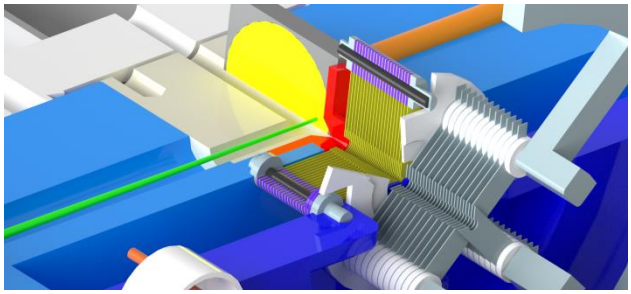

Figure 2. CAD-rendering of the setup design. Green: laser, yellow: target, red: nozzle, yellow and violet: RF-only funnel, grey and white: RF-buncher

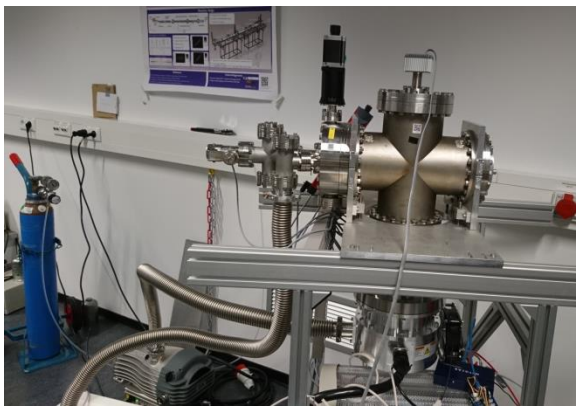

Figure 3. Current assembly connected to a CF 160 cross with a 900 l/s TMP and an 11 l/s Dry Piston Pump.

References

[1] D. Rodríguez, K. Blaum, W. Nörtershäuser et. al, MATS and LaSpec: High-precision experiments using ion traps and lasers at FAIR, Eur. Phys. J. Special Topics **183**, 1–123 (2010), DOI: 10.1140/epjst/e2010-01231-2.

[2] J. Krämer, K. König, et. al., Metrologia **55**, 268 (2018)

[3] Victor Varentsov, Proposal of a new Laser ablation ion source for LaSpec and MATS testing, NUSTAR Collaboration Meeting, 1 March, 2016, DOI: 10.13140/RG.2.2.10904.39686

Experiment beamline: none
Experiment collaboration: APPA-SPARC, NUSTAR-LASPEC
Experiment proposal: none
Accelerator infrastructure: CRYRING
PSP codes: none
Grants: HIC for FAIR, HGS-HIRE, BMBF 05P15RDFN1
Strategic university co-operation with: Darmstadt

 DOI:10.15120/GR-2018-1

Experimental determination of electron capture cross sections into excited states of decelerated xenon projectiles

F. M. Kröger[1,2,*], G. Weber[2,3], J. Glorius[3], Y. Litvinov[3,4], M. O. Herdrich[1,2], U. Spillmann[3], M. Vockert[1,2], Th. Stöhlker[1,2,3]

[1]FSU Jena, Germany; [2]HI Jena, Germany; [3]GSI, Germany; [4]RKU Heidelberg, Germany

Currently only very few data exists for electron-capture cross sections of highly-charged ions colliding with atoms/molecules at energies well below the respective projectile ionization threshold. However, such conditions will be common for beams of decelerated highly-charged heavy ions in the recently commissioned CRYRING@ESR of GSI/FAIR, Darmstadt, where the capture rate with residual gas atoms/molecules will determine the ion beam lifetimes. Thus, the knowledge of electron capture cross sections is of particular importance for the planning of experiments in this storage ring.

Here we report on the evaluation of experimental cross-section data obtained for Xe^{54+} ions colliding with H_2 molecules [1]. The experiment was performed at the internal gas target of the ESR storage ring at GSI, Darmstadt using collision energies between 5.5 MeV/u and 30.93 MeV/u. An array of Ge(i) X-ray detectors was placed at various observation angles around the interaction zone. These detectors allowed to record the X-ray emission arising from the ion-atom collisions, in particular those resulting from radiative capture of target electrons into bound states of the projectile ions and also characteristic K radiation due to subsequent transitions from excited states to the ground state, see fig. 1. Note that for a H-like high-Z system two-photon transition rates are negligibly small compared to single-photon transitions. Therefore, as all electron-capture events into excited states will lead to K transitions, the K-shell emission cross-section is a measure of the total electron capture cross-section into projectile states with $n > 1$. By normalizing the observed intensity of the characteristic K radiation to the K-REC (meaning Radiative Electron Capture into the projectile K-shell) intensity (similar to [2]) we related the characteristic K emission cross-section to the well-known K-REC angular differential cross-section.

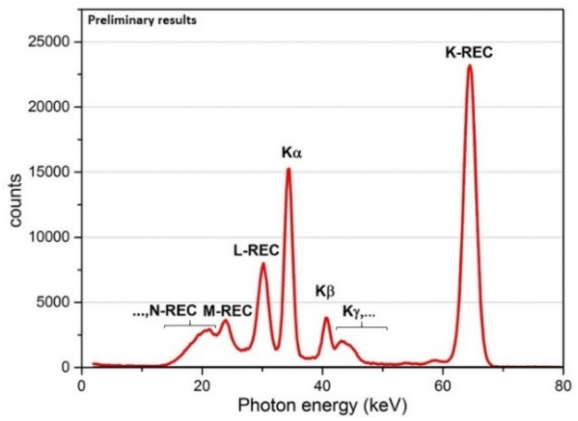

Figure 1: X-ray spectrum of bare xenon ions colliding with H_2 molecules at 30.93 MeV/u, recorded with a photon detector at 60°.

*felix.kroeger@uni-jena.de

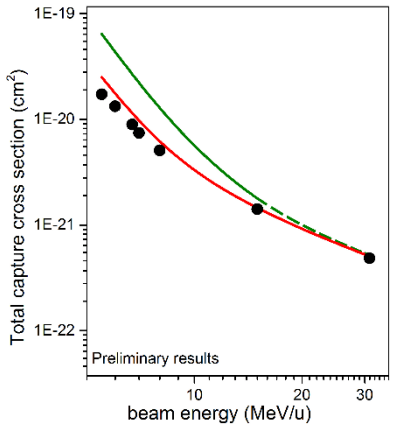

Figure 2: Comparison of total electron-capture cross-sections resulting as the sum of the REC cross sections from [3] and the NRC cross sections calculated with the Schlachter formula (green line) and with the eikonal theory (red line) to the experimental data (full circles) as function of the ion beam energy. In order to present total capture cross sections into all projectile states the experimental cross sections were complemented by theoretical K-REC cross sections.

In figure 2, a comparison of the commonly used empirical Schlachter formula (green line) [4] and of the eikonal theory [5] for non-radiative electron capture (NRC) plus the REC to the preliminary experimental data (full circles) is shown. For the particular collision system under discussion, the range of validity of the Schlachter formula is limited to $E_{kin} < 16$ MeV/u. A dashed line is used for beam energies that lie beyond this range. Note that for the operation of the CRYRING the most important parameters are the total electron capture cross-sections into all projectile states. Therefore, in order to compare the resulting experimental and the theoretical total electron capture cross-sections, theoretical K-REC cross-sections [3,6] were added to the experimental and theoretical capture cross sections into projectile states with $n > 1$. For completion also theoretical K-shell NRC cross-sections should be included, which however are negligibly small compared the K-REC cross-sections.

As can been seen in figure 2, the results of the Schlachter formula deviate markedly from the experimental data in contrast to the eikonal theory, which is in reasonable agreement with the experimental data.

[1] J. Glorius et al., JPCS 875, 092015 (2017).
[2] Th. Stöhlker et al., Phys. Rev. A 58(3), 2043 (1998).
[3] M. O. Herdrich et al., NIM B 408, 294 (2017).
[4] A. S. Schlachter et al. Phys. Rev. A, 27, 3372 (1983).
[5] J. K. M. Eichler, Phys. Rev. A 23, 498 (1981).
[6] G. Weber et al., JPCS 599, 012040 (2015).
[7] J. Eichler and Th. Stöhlker, Phys. Rep. 439, 1 (2007).

Towards laser spectroscopy of Mg^+ ions at CRYRING

K. Mohr[1], A.W. Barasa[1], Z. Andelkovic[2], A. Buß[3], V. Hannen[3], W. Nörtershäuser[1], T. Ratajczyk[1], R. Sánchez[2]

[1]Institut für Kernphysik, TU Darmstadt, Germany; [2]GSI, Darmstadt, Germany; [3]Institut für Kernphysik, WWU Münster, Germany

Storage ring experiments would tremendously benefit from polarized beams of stable and exotic nuclei, e. g. for experiments on parity violation. Therefore it has been suggested to polarize beams by optical pumping, which can be used to polarize the electron shell as well as the nucleus in the case of odd isotopes. However, it is not clear yet whether the induced polarization will persist during the revolution in the storage ring without additional means. On the round trip, the ions have to pass rapidly changing fields through the dipole and quadrupole magnets for deflection and focusing.

First evidence of the preservation of the polarization of an ion beam was found in our group during an experiment at the Experimental Storage Ring (ESR) to test special relativity [1]. A resonance signal was observed when irradiating the ion bunch by linearly polarized light. The resonance disappeared as soon as circularly polarized light (either σ^+ or σ^-) was used. In this case, the state with the highest magnetic quantum number m_F by using σ^+-light was occupied. Because there was no excited state with a magnetic quantum number $m_F' = m_F + 1$, no further excitation was possible and thus the fluorescence signal disappeared. However, systematic investigations are mandatory to prove the preservation of polarization carried in the electron shell during the round-trip.

Due to the vanishing nuclear spin there is no hyperfine splitting in $^{24}Mg^+$. This introduces $^{24}Mg^+$ as an ideal two-level candidate for these investigations. The $3\,^2S_{1/2} \leftrightarrow 3\,^2P_{1/2}$ transition at 280.35 nm could be used to populate the $m_s=+1/2$ sub-state, which is a dark state for further excitation with σ^+ light and thus realizing a polarization of the electron shell. The setup for such an experiment is ongoing.

To create $^{24}Mg^+$-ions, the local Nielsen-type ion source of CRYRING will be used. This local ion source was modified to accommodate an oven from which solids can be vaporized and fed into the plasma for ionization. From first tests we have observed $^{24}Mg^+$-ions with energies of 40keV and currents of about 10 µA before the injection into CRYRING. In the upcoming beam time at this storage ring it is planned to store and accelerate the Mg-ions up to 173 keV/u. Acceleration is mandatory to yield sufficient lifetimes of $^{24}Mg^+$-ions for the laser spectroscopy experiment.

One further experimental requirement is the efficient detection of the fluorescence light emitted by the excited ions. Fluorescence photons will be collected by using a combination of a mirror system mounted in vacuum together with sensitive photomultipliers (PMTs) [2]. The signal from the PMTs will be processed using photon tagging, a technique successfully used in previous laser experiments at ESR and TRIGA-LASER [3].

To ensure the common propagation direction of the laser beam and the ion beam, a scraper system has been installed in section YR07 (fig. 1). It will be used to check the ion beam's position in the horizontal and vertical direction and to superpose the ion and laser beams.

Figure 1: Scraper installation at section YR07.

Piezo-driven mirror-mounts positioned on turrets close to the coupling windows will be used to stabilize the laser beam in position. In addition, it can be used to adapt the position of the laser beam to the ion beam.

The laser laboratory has been completed and equipped with the required infrastructure including optical tables and laminar flow boxes. The laser transport from the lab to the coupling towers in section YR07 has been designed. The CRYRING cave is connected by a borehole to the laser lab. Breadboards for installation of optics like mirrors and some parts of the stabilization system have been mounted in the cave.

We will use a bunched beam to improve the signal-to-noise ratio. For data acquisition, TILDA [3] will be used. It is a time-resolved DAQ, which has been developed at the TRIGA-LASER setup [4] for laser spectroscopy on bunched and continuous beams. [3]. First tests of TILDA at the CRYRING facility will happen in 2018, to investigate and optimize scattered light background.

References

[1] M. Lestinsky et al., European Physical Journal: Special Topics 225, 797 (2016).
[2] see A. Buß *et al.*, this Annual Report.
[3] see S. Kaufmann *et al.*, this Annual Report
[4] C. Gorges, S. Kaufmann et al., Hyperfine Interactions 238, 1 (2017);

Experiment beamline: CRYRING
Experiment collaboration: APPA-SPARC
Experiment proposal: none
Accelerator infrastructure: CRYRING
PSP codes: 1.3.1.5.8.1.1
Grants: BMBF contract 05P15RDFAA, HIC4FAIR
Strategic university co-operation with: Darmstadt

 DOI:10.15120/GR-2018-1

Detectors and drives for UHV particle detection in CRYRING

A. Kalinin[1, 2], J. Glorius[1], C. Brandau[1,3], C. Langer[4], M. Lestinsky[1], Yu. A. Litvinov[1], S. Schippers[3], R. Reifarth[4], L. Varga[1], Y. Xing[1] and T. Stöhlker[1,2]

[1]GSI, Darmstadt, Germany; [2] HI Jena, Germany; [3] Justus-Liebig-Universität Gießen, Germany;
[4] Goethe Universität Frankfurt am Main, Germany;

Versatile detector drives for CRYRING

The design of new detector drives for the CRYRING@ESR facility based on the most recent detector drive installations in the ESR [1] has been finalized. The main concept behind the design is to have an ultra-high vacuum compatible detector chamber, which is separated from the ring vacuum by a gate valve. Thus, installation and bake-out of detectors is possible without disturbing the ring vacuum. A large variety of detection systems can be installed, as long as it can be adapted to the CF100 flange at the far end of the welded bellow. The system allows flexible positioning of the detectors with two types of drives: a stepping motor, used for slow and precise positioning and a pneumatic actuator that can be used for fast and automated movement.

The drives come in two different lengths as shown in Fig.1. The long version provides a stepping motor travel of 70 cm, which is needed to cover the full acceptance inside the dipole chambers. A shorter version with a travel of 35 cm is sufficient for direct connection to the beam pipe.

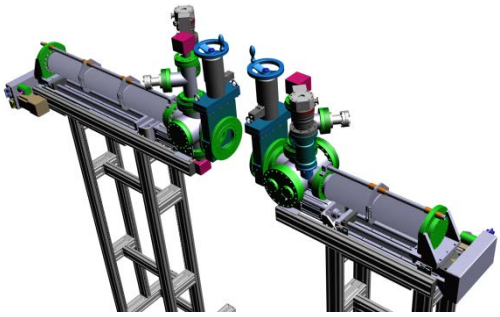

Figure 1: CAD drawing of the long version (left side) and the short version (right side) of the new detector drives.

A new dipole chamber for section YR09/10

In order to register ions from ionization and electron capture (or equivalent) processes for low charge states at the internal target of CRYRING, a large acceptance directly behind the next dipole is needed. The dipole chamber installed behind the electron cooler served as a basis for a new design of a similar chamber. The new chamber has been already built (Fig. 2) and vacuum tested at GSI.

Figure 2: The new dipole chamber at first inspection in the UHV lab of GSI before the vacuum tests.

A fast particle detector for UHV environment

To fulfil the experimental demands of the CRYRING and to meet the technical design requirements of the detector drives, a suitable detector system has been designed, manufactured and tested. The detection scheme is based on surface secondary-electron emission with subsequent multiplication in an channel electron multiplier (CEM) [2]. The detector head is mounted on a > 1m long supporting holder arm with appropriate electrical connections.

Implementation of an extended dynamic range channel electron multiplier, in the current design, improves the performance of the detector for count rates up to 15 MHz, as it was verified with up to 2 MeV singly charged argon ions from the Van-de-Graaff accelerator at IKF, Frankfurt.

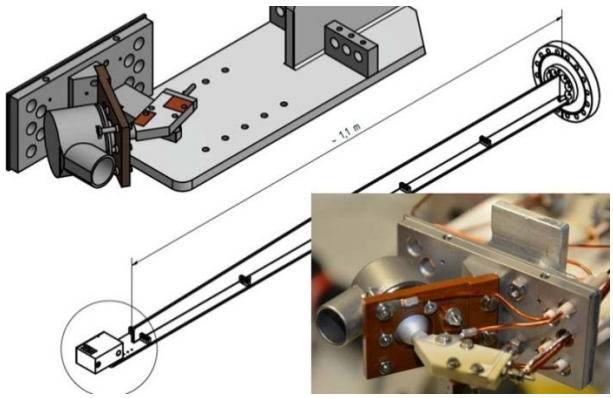

Figure 3: CAD drawings of the detector construction (top left), detector's holder arm (middle) and photo of the detector assembly without protection housing (bottom right).

References

[1] Brandau et al., GSI scientific report 2013, p. 160.
[2] Rinn et al., Rev. Sci. Instr. 53 (1982) p. 829.

Experiment beamline: CRYRING
Experiment collaboration: APPA-SPARC
Experiment proposal: none
Accelerator infrastructure: CRYRING
PSP codes: 1.3.1.5.7.1
Grants:
- BMBF 05P15RFFAA
- EU H2020 contract No. 682841 "ASTRUm"
Strategic university co-operation with:
- Goethe Universität Frankfurt am Main;
- Justus-Liebig-Universität Gießen;

Measurements of linear polarization of radiative electron capture*

M. Vockert[1,2], G. Weber[2,3], U. Spillmann[3], T. Krings[4] and Th. Stöhlker[1,2,3]
for the SPARC Collaboration

[1]Friedrich Schiller University, Jena, Germany; [2]HI Jena, Germany; [3]GSI, Darmstadt, Germany; [4]FZ Jülich, Germany

In recent years, substantial efforts of the SPARC collaboration went into the development of Compton polarimeters to address the linear polarization properties of hard x-rays emitted by relativistic highly-charged ions interacting with matter. By applying this technique, subtle effects could already be revealed such as the E1/M2 multipole mixing for the linear polarization of the Lyman transitions in H-like uranium [1] or the polarization transfer of bremsstrahlung arising from spin-polarized electrons [2]. Moreover, recently the polarization transfer in Rayleigh scattering was studied using the aforementioned polarimeter systems [3]. To further improve and to widen the range for future applications, a new 2D position-sensitive demonstrator system has been developed based on a ≈9 mm thick Li-drifted silicon detector (for details see Ref. [4]). The unique feature of this new demonstrator is cooled preamplifiers, enabling a strong noise reduction and consequently a substantial improvement of the energy resolution.

The superior performance of the new polarimeter system was demonstrated in a test experiment at the internal gas target of the ESR storage ring. For the measurement, bare xenon ions at an energy of 31 MeV/u have been used, colliding with a molecular hydrogen target [5]. The x-ray emission associated with electron capture into the projectile ions has been observed at 90° with respect to the beam axis in coincidence with a particle detector located behind the next dipole magnet. The resulting well-resolved x-ray spectrum is displayed in figure 1, showing radiative electron capture (REC) as well as characteristic transitions of the projectile.

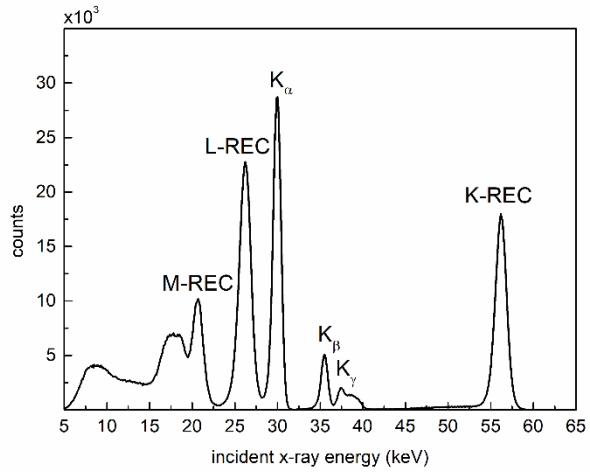

Figure 1: Spectrum obtained at the internal gas target of the ESR storage ring at 90° observation angle using a beam of bare xenon ions at a kinetic energy of 31 MeV/u and a hydrogen target.

Due to the improved detector performance, Compton polarimetry could be applied to the K-REC radiation with an energy of about 56 keV. Note that when using the previous Compton polarimeters with preamplifiers at room temperature, this technique could only be applied at energies above 80 keV.

The preliminary analysis indicates an almost complete linear polarization (close to 100%, see Fig. 2). This finding is in agreement with rigorous relativistic calculations which for the specific collision system and observation angle yield similar results as the non-relativistic dipole approximation [6]. This observation indicates that for medium-Z ions and at such low collision energies, relativistic effects are quite small. Note, in comparison with the data previously obtained at higher energies [7,8], the obtained accuracy of the improved polarimeter is significantly higher, leading to an uncertainty in the degree of linear polarization of only about 1.5%. In addition, we would like to note that by utilizing the characteristics of the REC radiation, we realize an energy-tunable, monochromatic source of almost fully polarized x-rays for a broad energy range.

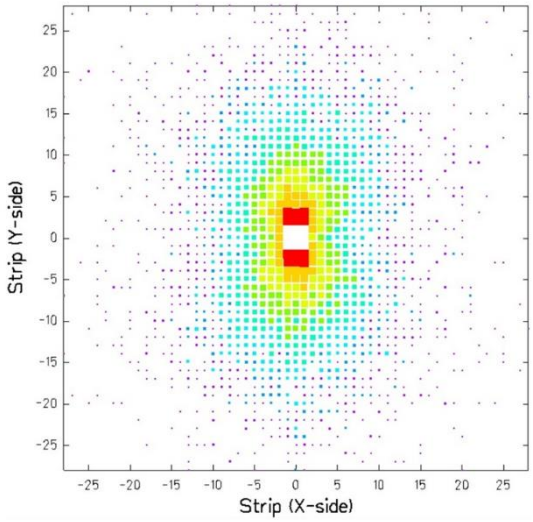

Figure 2: Position distribution of the scattered Compton photons with respect to the point where the scattering took place for the K-REC peak restricted to polar scattering angles of $\vartheta = (90 \pm 15)°$.

[1] G. Weber et al., Phys. Rev. Lett. 105, 2010, 243002
[2] R. Märtin et al., Phys. Rev. Lett 108, 2012, 264801
[3] K.-H. Blumenhagen et al., New J. Phys. 18, 2016, 103034
[4] M. Vockert et al., Nucl. Instr. Meth. B 408, 2017, 313
[5] J. Glorius et al., J. Phys. Conf. Ser. 875, 2017, 092015
[6] J. Eichler and Th. Stöhlker, Phys. Reports 439, 2007, 1-99
[7] S. Tashenov et al., Phys. Rev. Lett. 97, 2006, 223202
[8] S. Hess et al., J. Phys. Conf. Ser. 194, 2009, 012205

* Work supported by BMBF Verbundprojekt 05P15SJFAA. This report is also part of the HI Jena Scientific Report 2017.

 DOI:10.15120/GR-2018-1

Ground-state ionization energies of boronlike ions

A. V. Malyshev[1,2], D. A. Glazov[1,3], A. V. Volotka[1,4], I. I. Tupitsyn[1,5], V. M. Shabaev[1], G. Plunien[6], and Th. Stöhlker[4,7,8]

[1]St. Petersburg State University, St. Petersburg, Russia; [2]ITMO University, St. Petersburg, Russia; [3]SSC RF ITEP of NRC „Kurchatov Institute“, Moscow, Russia; [4]Helmholtz-Institut Jena, Jena, Germany; [5]Peter the Great St. Petersburg Polytechnic University, St. Petersburg, Russia; [6]Technische Universität Dresden, Dresden, Germany; [7]GSI, Darmstadt, Germany; [8]Friedrich-Schiller-Universität, Jena, Germany

State-of-the-art quantum electrodynamics (QED) calculations of the energy levels in highly charged ions include all relevant contributions up to the second order in α, see, e.g., Refs. [1,2] for theory concerning H- and He-like heavy ions. High-precision measurements of the binding and transition energies which are sensitive to the second-order corrections [3-6] con rm predictions made by QED theory to a high level of accuracy and allow one to test bound-state QED in the strong- eld regime. Nevertheless, the precision currently reached in the strong eld domain of high-Z ions is still much less as compared to the one for light atoms and thus a further extension and improvement of *ab initio* QED calculations are of great importance.

The present investigation [7] is focused on ve-electron (boronlike) ions. Namely, we perform high-precision QED calculations of the ground-state ionization energies for all boronlike ions with the nuclear charge numbers in the range $16 \le Z \le 96$. The developed rigorous QED approach includes all many-electron QED e ects up to the second order of the perturbation theory. The contributions of the third- and higher-order electron-correlation e ects are accounted for within the Breit approximation by means of the con guration-interaction Dirac-Fock-Sturm method [8] and alternatively employing the recursive formulation of the perturbation theory [9]. The nuclear recoil and nuclear polarization e ects are taken into account as well. All the calculations are carried out in the framework of the extended Furry picture starting with several di erent types of the screening potential. The deviations of the nal results obtained with the use of di erent zeroth-order approximations are employed in order to estimate the uncalculated higher-order QED contributions.

The results obtained are presented in Table 1 for selected boronlike ions. Our theoretical predictions for the ionization energies are compared with the results obtained by other groups [10-13]. One can see, that our results are in good agreement with the results of the previous relativistic calculations. However, the accuracy of the theoretical predictions is improved signi cantly.

Finally, we note, that taking into account the results of [14] one can easily obtain the ionization energies for the rst excited state of boronlike ions; for this one needs to add the transition energies presented in [14] to the ground-state ionization energies evaluated in this work.

Nucleus	This work [7]	Other works	Ref.
^{40}Ca	-973.7863(53)	-973.70(33)	[10]
		-973.83	[11]
		-973.84(29)	[12]
^{56}Fe	-1798.7978(63)	-1798.43(78)	[10]
		-1798.8	[11]
^{132}Xe	-9238.499(20)	-9238.2	[11]
		-9243(4)	[13]

Table 1: Ionization energies (in eV) for boronlike ions.

References

[1] V. A. Yerokhin and V. M. Shabaev, J. Phys. Chem. Ref. Data 44 (2015) 033103.
[2] A. N. Artemyev *et al.*, and G. Soff, Phys. Rev. A 71 (2005) 062104.
[3] A. Gumberidze *et al.*, Phys. Rev. Lett. 92 (2004) 203004.
[4] C. Brandau *et al.*, Phys. Rev. Lett. 91 (2003) 073202.
[5] P. Beiersdorfer *et al.*, Phys. Rev. Lett. 95 (2005) 233003.
[6] K. Kubiček *et al.*, Phys. Rev. A 90 (2014) 032508.
[7] A. V. Malyshev *et al.*, Phys. Rev. A 96 (2017) 022512.
[8] I. I. Tupitsyn *et al.*, Phys. Rev. A 68 (2003) 022511.
[9] D. A. Glazov, Nucl. Instr. Meth. Phys. Res. B 408 (2017) 46.
[10] E. Biémont *et al.*, At. Data Nucl. Data Tables 71 (1999) 117.
[11] M. F. Gu, At. Data Nucl. Data Tables 89 (2005) 267.
[12] N. N. Dutta and S. Majumder, Phys. Rev. A 85 (2012) 032512.
[13] G. C. Rodrigues *et al.*, At. Data Nucl. Data Tables 86 (2004) 117.
[14] A. N. Artemyev *et al.*, Phys. Rev. A 88 (2013) 032518.

Experiment collaboration: APPA-SPARC

Grants: SPSU-DFG (No. 11.65.41.2017 and No. STO 346/5-1)

Strategic university co-operation with: St. Petersburg State University

The spectral shape of the atomic two-photon transition in He-like ions

S. Trotsenko[1], A. Volotka[2,3], A. Surzhykov[4,5], A. Kumar[6], D. Banas[7], A. Gumberidze[8], H.F. Beyer[8], H. Bräuning[8], S. Fritzsche[1,2], S. Hagmann[8,9], S. Hess[8], P. Jagodzinski[7], C. Kozhuharov[8], R. Hess[8], S. Salem[8], A. Simon[10], U. Spillmann[8], M. Trassinelli[11], L.C. Tribedi[12], G. Weber[2,8], D. Winters[8], and Th. Stöhlker[1,2,8]

[1]Friedrich-Schiller-Universität, Jena, Germany; [2]Helmholtz Institute Jena, Jena, Germany; [3]Department of Physics, St. Petersburg State University, St. Petersburg 198504, Russia; [4]Physikalisch-Technische Bundesanstalt Braunschweig Germany; [5]Technische Universität Braunschweig Braunschweig Germany; [6]NPD, Bhabha Atomic Research Centre, Mumbai, India; [7]IP, Jan Kochanowski University, Kielce, Poland; [8]Helmholtzzentrum GSI, Darmstadt, Germany; [9]IKF, University of Frankfurt, Frankfurt, Germany; [10]Department of Physics, University of Notre Dame, Notre Dame, IN 46556, USA; [11]Institut des NanoSciences de Paris, CNRS, Sorbonne Universités, UPMC Univ Paris 06, F-75005 Paris, France; [12]Tata Institute of Fundamental Research, Homi Bhabha Road, Coloba, Mumbai 400005, India

Two-photon decay has been an interesting topic since its prediction in 1930's by M. Göppert-Mayer [1]. In this process, two correlated photons are emitted simultaneously under the boundary condition that the sum of their energies equals to the total transition energy, i.e.

$$\hbar\omega_1 + \hbar\omega_2 = E_I - E_F = E_0 \qquad (1)$$

Here, $\hbar\omega_1$ and $\hbar\omega_2$ are the energies of the photons, E_0 is the total transition energy, and E_I and E_F are the energies of initial and final atomic states, respectively. The energies of individual photons form a continuum spectrum which, for the case of decay from $2s$ state, has a maximum intensity at half of the transition energy and gradually falls to zero at both endpoints. This continuum shape is determined by the summation over all intermediate bound- and continuum-states for calculating the transition probabilities which requires knowledge of their energies and wave functions. Hence, the spectral distribution of the two-photon emission is sensitive to the entire atomic structure.

Measurements of the two-photon spectral shape in He-like ions have been significantly improved by the method involving a selective ionisation of a K-shell electron from the initially Li-like ion [2]. Using this method a very clean spectral distribution of the 2E1 decay of $2\,^1S_0$ in He-like tin has been measured. From the measured distribution, a reduced full width at half maximum (FWHM) was obtained. For this, the experimental distribution was fitted with a polynomial distribution. The reduced FWHM was calculated as the width of the distribution divided by the maximum possible photon energy (the energy difference between the $1s2s\ ^1S_0$ and $1s^2\ ^1S_0$ states).

Our preliminary result for the reduced FWHM is compared with theoretical values in figure 1. The comparison shows a clear deviation from the non-relativistic prediction and a very good agreement with our relativistic calculations based on the method developed in [3]. This unambiguously confirms the importance of the relativistic effects for the 2E1 two-photon decay energy distribution. Here, we would like to add that the relativistic values for FWHM obtained by Derevianko and Johnson [4] were found to be in good agreement with the results of our relativistic calculations [2]. The current experimental value for He-like tin can be considered to favor the fully relativistic treatment against the frozen Dirac-Fock result, thus emphasising the importance of accurate treatment of the electron-electron interaction in the mid-Z regime.

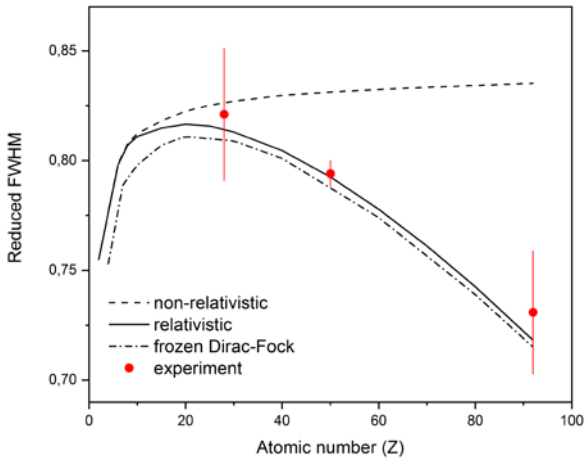

Figure 1: Preliminary results: Comparison of the measured reduced FWHM of the 2E1 two-photon spectral shape for He-like tin with the nonrelativistic calculations (dashed line), the frozen Dirac-Fock method (dashed-dotted line) and the relativistic calculations (solid line). In addition, the experimental values for He-like nickel [5] and uranium [6] are shown.

References

[1] M. Göppert-Mayer, Naturwissenschaften 17, 932 (1929)
[2] S. Trotsenko et al., Phys. Rev. Lett. 104, 033001 (2010).
[3] A. V. Volotka, A. Surzhykov, V.M. Shabaev, and G. Plunien, Phys. Rev. A 83, 062508 (2011).
[4] A. Derevianko, W. R. Johnson, Phys. Rev. A 56, 1288 (1997).
[5] H. W. Schäffer et al., Phys. Scr. T80, 469 (1999).
[6] D. Banas et al, Phys. Rev. A 87, 062510 (2013).

Experiment beamline: ESR
Experiment collaboration: APPA-SPARC
Accelerator infrastructure: ESR
Strategic university co-operation with: FSU Jena

*Also part of the HI-Jena scientific report 2017

 DOI:10.15120/GR-2018-1

First tests of x-ray crystal optics at the S-EBIT facilities

S.Wipf,[1,2], S.Trotsenko[1], Robert Lötzsch[1], R. Schuch[3], Th. Stöhlker[1,2]

[1]Friedrich-Schiller-Universität Jena, Germany; [2]HI Jena, Germany; [3]University of Stockholm

Studies at Electron Beam Ion Traps (EBIT) have gained large interest in particular in the domain of atomic physics and astrophysics. Here, majority of experiments are based on x-ray spectroscopy of the trapped ions. Thereby one can acquire detailed knowledge about transitions in partially ionized atomic systems and also gain information on the physical processes in EBITs to make statements particularly concerning the ion charge-state distributions. In such x-ray spectroscopic studies, the energy resolution plays certainly a very important role.

The S-EBIT facility of the Helmholtz Institute Jena, apart from other activities, provides a tool for further steps in the improvement of x-ray spectroscopy in terms of resolving power and collection efficiency. Our previous x-ray diagnostics at the S-EBIT was so far based on a silicon (or germanium) pin-diode detectors with a resolution of a few 100 eV in the energy region of interest [1].

Magnetic metallic microcalorimeters possess new very promising x-ray detection technology that combines the excellent spectral resolution being typical for crystal spectrometers with the high stopping power of solid-state detectors. With this detector technology, the resolution for photon energies in keV range can be as good as a few eV [2]. But, such microcalorimeters usually provide only a small active area and, consequently, can cover only a small solid angle, in particular if the high magnetic field of the EBIT limits the geometry. Here, the application of focussing x-ray crystal optics becomes handy and the effective surface of the detector can be increased by at least an order of magnitude (Fig. 1). The incident and the outgoing x-rays should fulfil the Bragg condition for the x-ray energies that are subject to enhanced detection efficiency. For the details of this technology we refer to [3].

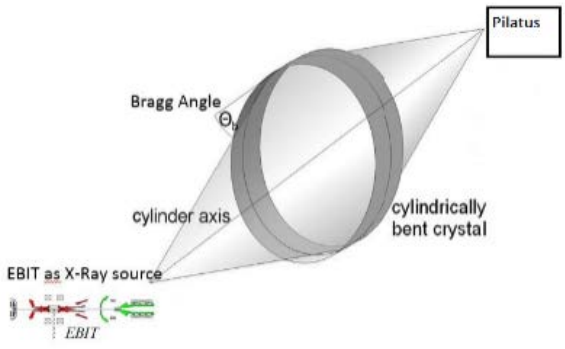

Figure 1: A sketch of the set up and crystal optics mounted in front of the EBIT together with a position sensitive Pilatus detector.

Here we present a first proof of principle measurement with the aforementioned method. The K_α-line of iron ions was observed at around 6.75 keV. The crystal optics we used is made of Highly Annealed Pyrolitic Graphite (HAPG) and modified for reflection in the energy range from 7 keV to 12.5 keV. We used a spatial resolving silicon pixel detector PILATUS behind the toroidal shaped x-ray optics and obtained an image of the ion cloud inside the trap. A motorized steering with dedicated LabView software was used to align the x-ray optics to match the focussing conditions, given by the energy-dependent Bragg angle and the distance between source, optics and the detector. The threshold of the Pilatus detector was set to 1.5 keV and frames with 100 s exposure time were taken. Figure 2 (top) shows an image of the ion trap in the x-ray wavelength- range with the presented set up and a corresponding energy spectrum measured with a Si-pin diode on the opposite view port of the trap (bottom). The EBIT-I operated with 25mA (10keV) electron beam.

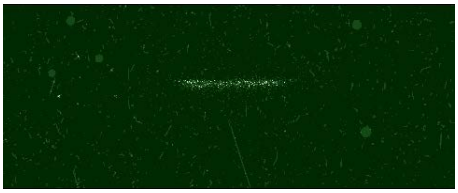

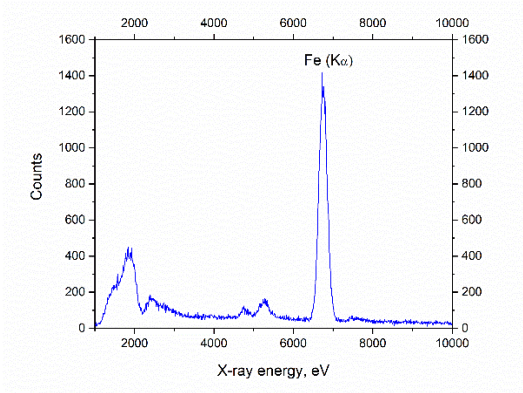

Figure 2: Image of the EBIT x-rays formed by the x-ray optics (top) and a spectrum measured in parallel with the Si-pin diode (bottom).

The further steps are currently in progress and will involve measurements with a position and energy resolving CCD detector. Ultimately, a combination of the magnetic metallic microcalorimeter detectors with the crystal optics at the S-EBIT should reveal the full power of the invented method for x-ray spectroscopy of highly charged ions.

References

[1] S. Trotsenko, HI Jena Scientific Report 2016, p.76
[2] C. Pies et al., 2012, J Low Temp Phys (2012) 167:269–279
[3] R. Lötzsch, HI Jena Scientific Report 2015, p. 49

Experiment collaboration: APPA-SPARC
PSP codes: [none]
Strategic university co-operation with: FSU Jena

*Also a part of the HI-Jena scientific report 2017

Status of the data analysis from proton capture reaction measurement with a UHV compatible DSSSD

L. Varga[1], T. Davinson[2], J. Glorius[1], C. Langer[3], Yu. A. Litvinov[1], R. Reifarth[3], Z.Slavkovska[1], T. Stöhlker[1,2], P. J. Woods[2], Y. Xing[1] and NuCAR Collaboration

[1]GSI, Darmstadt, Germany; [2]University of Edinburgh, UK; [3]Goethe Universität Frankfurt am Main, Germany

In 2016, the very first measurement of the ^{124}Xe(p,γ)^{125}Cs proton capture reaction was performed at Experimental Storage Ring (ESR) at GSI. A beam of stable fully-stripped $^{124}Xe^{54+}$ ions was stored at five different energies, from 10 MeV/u to 5.5 MeV/u. The aim was to measure the absolute cross section [1].

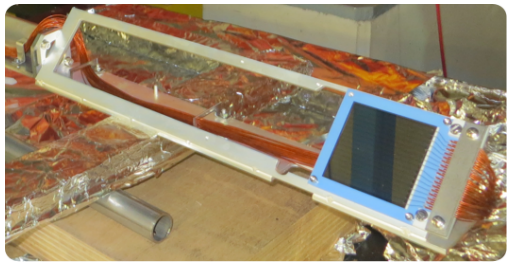

Figure 1: A photo of the UHV compatible DSSSD used in the experiment.

For the measurement at such low energies, the use of Ultra High Vacuum (UHV) proof detectors due to the excellent vacuum conditions of the ESR (10^{-11} mbar) was indispensable. The required UHV compatibility was ensured by the special design of a double sided silicon strip detector (DSSSD) with nearly 100% particle detection efficiency for heavy ions at ESR energies (see Fig. 1).

Due to the x and y segmentation of the DSSSD realized by 16 silicon strips on both, the front and back side of the detector (perpendicularly aligned), spacial resolution of the reaction products can be achieved. The proton capture products can be recognized as a narrow cluster of events on the top of the background signal due to the elastically scattered ions as shown in Figure 2. In order to determine the absolute cross section of the (p,γ) reaction, the number of hits in the proton capture cluster should be identified. However, to achieve high detection efficiency for Highly Charged Ions (HCI) a clear separation between the ion and the noise events is essential. For this, the excellent energy resolution of the silicon detector can be utilized. In Figure 3 the energy spectrum of one strip of the DSSSD is visible. In the energy distribution, three different types of events can be distinguished: close to 0 energies is the noise peak, at the higher-end of the distribution is the ion peak, and between these two peaks are the so-called interstrip (IS) events. In case of IS events, the charge produced by an ion hit is shared between two adjacent Si strips. In order to provide a better separation between the noise and the ion peak, the energy of the IS hits should be reconstructed by summing up the energies of the neighboring strips event by event. After the reconstruction, a narrow acceptance window close to the ion-peak energy can be applied to select the events of interest.

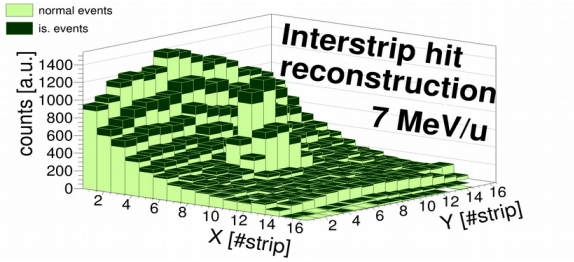

Figure 2: Spacial distribution before and after IS hit reconstruction

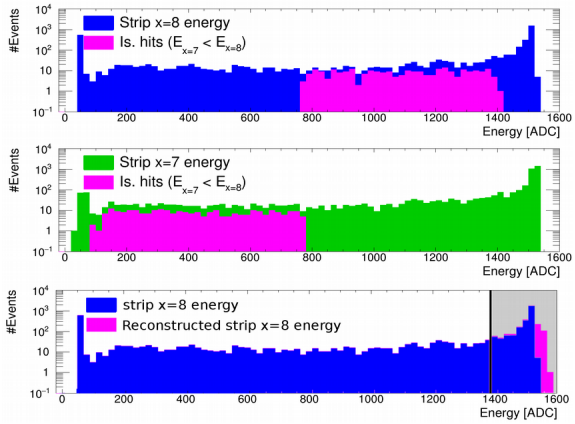

Figure 3: Top and middle panels: energy spectra of two adjacent strips. Bottom figure: energy spectrum of a strip before and after IS hit reconstruction

In Figure 2 the spatial distribution of the DSSSD hits at 7 MeV/u is visible before and after the interstrip hit reconstruction. In case of a narrow acceptance window, the reconstructed interstrip hits have considerable impact on the total number of events. The average ratio between the single-strip events (light green) and the interstrip events (dark green) reaches ~15%.

References

[1] J.Glorius et. al., J. Phys: Conf. Ser 875 (2017)092015.

Experiment beamline: ESR
Experiment collaboration: APPA-SPARC
Experimental proposal: E108
Accelerator infrastructure: ESR

Grant: EU H2020 contract No. 682841 "ASTRUm"

 DOI:10.15120/GR-2018-1

Progress of a variable sensitivity resonant Schottky pick-up cavity

M. S. Sanjari[1], O. Gumenyuk[1], D. Dmytriiev[1,2], Ch. Kozhuharov[1], Yu. A. Litvinov[1,2] and Th. Stöhlker[1,3]

[1]GSI, Darmstadt; [2]Universität Heidelberg; [3]Helmholtz-Institut Jena

Schottky pickups are indispensable at accelerators. They can as well be designed to meet specific needs for performing precision atomic and nuclear physics experiments with stored highly-charged ions (HCI) in storage rings. In this work, we report on the progress of our latest developments at GSI.

The passage of particles through non-destructive electromagnetic detectors in storage rings induces a periodic signal that can be related to the particle's mass through its revolution frequency. Additionally, the recorded signal can deliver information on the lifetime of the unstable nuclei if the data is processed through short time Fourier analysis. Furthermore, these so called Schottky signals deliver information on general properties of the particle beam such as momentum spread [1] and can even be used to observe stability of other elements in the storage ring such as the electron cooler [2] and magnet power supplies.

Electromagnetic detectors designed for the detection of Schottky signals are based on a variety of geometries with their respective advantages and disadvantages for each application [3]. Of particular interest for precise determination of particle frequencies and intensities in storage rings are resonant cavities. Due to their high Q value, they can achieve high sensitivities, albeit at the cost of lower operation bandwidth. The usually large eigenmode frequency also allows for higher frequency and hence higher mass resolution power. One such detector has been developed for the ESR storage ring at GSI facility [4] and its single ion sensitivity has been demonstrated [5].

An R&D prototype of a longitudinally sensitive resonant Schottky cavity has been constructed and delivered to GSI. It is designed for the Collector Ring (CR) and High Energy Storage Ring (HESR) of the future FAIR project as a part of ILIMA and SPARC collaborations. The technical design report (TDR) has been prepared [6].

The new detector will allow for on-line variation of its sensitivity during the operation. This is achieved by means of mode dependent loading and by inserting dispersive material. This feature would extend the scope of application of resonant cavity detectors in future storage ring experiments.

All frequency tuner drives are controlled by standard FAIR components and hence compatible with FAIR control system. It is planned to test the prototype in the ESR. To this end, the cavity is currently undergoing various electromagnetic and vacuum tests. Further studies regarding the Data acquisition will employ Software Defined Radio (SDR).

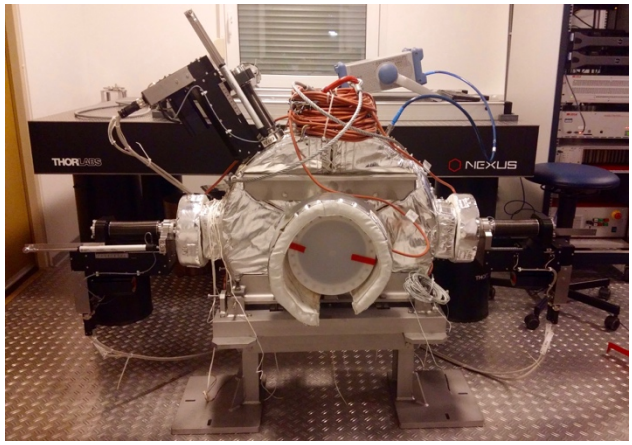

Figure 1: The prototype Schottky detector under test.

Acknowledgements

M. S. S. Would like to thank many colleagues involved in the preparation and construction of this prototype: J. Häuser, (Kress GmbH), H. E. Durand-Paredes, E. Keller, I. Schurig, W. Sturm, O. Zurkan (mechanical integration, K. Dermati, J. Holluba, M. Rosan, M. Romig, S. Teich, T. Schneider, (mechanical construction), D. Acker, M. Bevcic (Infrastructure), M. C. Bellachioma, J. Cavaco Da Silva, Ch. Kolligs, J. Kurdal, E. Renz, G. Savino, M. P. Suherman, L. Urban (vacuum systems) and Z. Fekete, R. Vincelli (IT) and M. Steck (ESR) and the ILIMA and SPARC collaboration members.

References

[1] F. Caspers 2009 CERN-2009-005.407
[2] S. Sanjari et al. GSI Sci. Rep. 2015 p 335
[3] G. R. Lambertson 1989 ISBN 978-3662137116
[4] F. Nolden et al. 2011 NIM A v 659 pp 69-77
[5] F. Bosch et al. 2013 Phys.Lett.B v1726 pp638-645
[6] S. Sanjari et al. 2017 TDR Schottky Detector System

Experiment beamline: ESR
Experiment collaboration: APPA-SPARC / NUSTAR-ILIMA
Experiment proposal: none
Accelerator infrastructure: ESR, CR, HESR
PSP codes: 1.2.6.3 and 1.3.1.3.12
Grants: ERC-2015-CoG (ASTRUm - 682841)
Strategic university co-operation with: Heidelberg

Excitation of helium-like uranium in relativistic collisions

A. Gumberidze[1], D.B. Thorn[2,], A. Surzhykov[3,4], C.J. Fontes[5], H.L. Zhang[5], B. Najjari[6], A. Voitkiv[7] , S. Fritzsche[8,9], D. Banas[10], H.F. Beyer[11], W. Chen[12], R. E. Grisenti[11,13], S. Hagmann[11,13], R. Hess[11,], P.-M. Hillenbrand[14,], P. Indelicato[15,], C. Kozhuharov[11], M. Lestinsky[11,], R. Märtin[8,11,], N. Petridis[11,], R. Popov[16,], R. Schuch[17], U. Spillmann[11], S. Tashenov[18], S. Trotsenko[8,9], A. Warczak[19], G. Weber[8,11], W. Wen[20], D.F.A. Winters[11], N. Winters[11], Z. Yin[21] and Th. Stöhlker[8,9,11]

[1]ExtreMe Matter Institute EMMI and Research Division, GSI Darmstadt, Germany; [2]LLNL, Livermore, California, USA; [3]Physikalisch-Technische Bundesanstalt, Braunschweig, Germany; [4]Technische Universität Braunschweig, Germany; [5]Computational Physics Division, LANL, Los Alamos, USA; [6]Institut Pluridisciplinaire Hubert-Curien, Strasbourg, France; [7]Heinrich-Heine-University of Düsseldorf, Germany; [8]Helmholtz-Institut Jena, Germany; [9]Friedrich-Schiller-Universität Jena, Germany; [10]Jan Kochanowski University, Kielce, Poland; [11]GSI Darmstadt, Germany; [12]Chinese Academy of Sciences, Institute of High Energy Physics, Dongguan, China; [13]Goethe-Universität, Frankfurt am Main, Germany; [14]Columbia University, New York City, USA; [15]Laboratoire Kastler Brossel, UPMC, CNRS, ENS-PSL Research University, College de France, Paris, France; [16]St. Petersburg State University, Russia; [17]Stockholm University, Sweden; [18]Ruprecht-Karls-Universität Heidelberg, Germany; [19]Jagiellonian University, Krakow, Poland; [20]Institute of Modern Physics, Chinese Academy of Sciences, Lanzhou, China; [21] DESY, Hamburg, Germany

In this contribution, we present an experimental and theoretical study of the K-shell excitation in helium-like uranium in relativistic collisions with different gaseous targets. The experiment was conducted at the experimental storage ring ESR. Around 10^8 U^{90+} ions produced by successive acceleration and stripping were stored and cooled in the ESR. For the measurement, the internal supersonic jet target was used crossing the beam in a perpendicular direction. The used target areal densities were between 10^{13} and 10^{14} particles/cm^2 and the interaction zone was defined by an overlap of the cooled ion beam (diameter ~2 mm) with the jet target (diameter ~6 mm). The projectile excitation process was explored by looking at characteristic X-rays emitted during the decay of the excited L-shell levels. For this purpose, we used the atomic physics experimental chamber at the internal target of the ESR. More details concerning the experimental setup and data analysis can be found in [1,2]

The experiment was performed with H_2 and Ar targets and two different beam energies of 218 MeV/u and 300 MeV/u. By performing measurements with different targets as well as with different collision energies, we were able to gain access to both; proton (nucleus) impact excitation (PIE) and electron impact excitation (EIE) processes in the relativistic collisions [1,2]. These beam energies have been chosen to be near and well above the EIE threshold. The cross sections for the two processes scale as Z^2_T and Z_T , respectively (Z_T being the target atomic number). Therefore, the relative contribution of the EIE is largest for hydrogen target.

In table 1, we present a comparison of our experimental results for intensity ratios of the characteristic Kα lines with state-of-the-art theoretical predictions based on the methods outlined in [3,4]. From the comparison it can be stated that the experimental results can be reproduced well by the fully relativistic calculations taking into account both PIE and EIE processes. Only PIE calculations significantly deviate from the experimental results even for the Argon target. It should be noted that the comparison is still preliminary because the possible influence of cascade contributions due to the excitation to higher levels as well as the possible role of the Compton profile of the bound target electrons have still to be assessed.

	218 MeV/u		**300 MeV/u**	
	H_2	Ar	H_2	Ar
Experiment	0.92 ± 0.02	1.33 ± 0.03	1.03 ± 0.03	1.39 ± 0.02
PIE+EIE	0.89	1.38	1.08	1.41
PIE	1.47	1.47	1.46	1.46

Table 1. Experimental results in comparison with theoretical predictions for $K\alpha_1/K\alpha_2$ intensity ratios for the K-shell excitation of U^{90+} in collision with H_2 and Ar targets at 218 MeV/u and 300 MeV/u.

References

[1] A. Gumberidze at al., Phys. Rev. Lett. 112, 213201 (2013).

[2] A. Gumberidze et al., J. Phys. B: At. Mol. Opt. Phys. 48, 144006 (2015)

[3] A. Surzhykov at al., Phys. Rev. A 77, 042722 (2008).

[4] C. J. Fontes, D. H. Sampson, and H. L. Zhang, Phys. Rev. A 47, 1009 (1993).

Experiment beamline: ESR
Experiment collaboration: APPA-SPARC
Experiment proposal: E101
Accelerator infrastructure: ESR
PSP codes: [none]
Grants: [This work was supported by the Helmholtz Alliance Program of the Helmholtz Association, Contract No. HA216/EMMI ‘‘Extremes of Density and Temperature: Cosmic Matter in the Laboratory.’’]
Strategic university co-operation with: Frankfurt-M / Jena]

 DOI:10.15120/GR-2018-1

Mode-dependent loading of resonant pick-up cavities

D. Dmytriiev[1,2], M. S. Sanjari[1], Yu. A. Litvinov[1,2], Th. Stöhlker[1,3]

[1]GSI, Darmstadt; [2] Universität Heidelberg; [3]Helmholtz Institut Jena

Non-destructive Schottky spectroscopy is a widely used technique in experiments at storage rings. While passing through the cavity, beam induces mirror charges on the inner surface of the cavity and one can use oscillations of the excited electromagnetic field inside the cavity as a signal source. Due to losses in materials, oscillations of the electromagnetic field inside the cavity will be damped. Therefore, one can imagine the resonant cavity as a parallel RLC circuit (Figure 1) where M_1 is the coupling between the beam and the electromagnetic field inside the cavity, R – real part of the cavity impedance, L – inductivity of the cavity, C – electrical capacitance of the cavity. M_2 and M_3 are the couplings related to the coupler of the external read-out circuit and additional loading.

The main subject of this work is to investigate the influence of external loading on the loaded quality factor of the cavity. The reason is that the cavity should have a negligible influence on the ion beam while other experiments are running in the storage ring but also work as a detector when it is needed. To change intensity of interaction between the cavity and the beam, one can use mode-dependent loading.

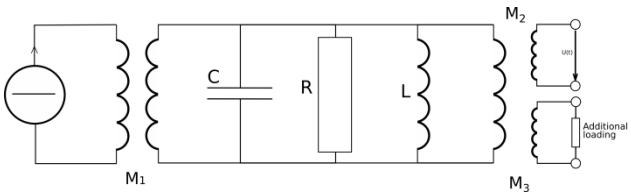

Figure 1: Equivalent circuit of the resonant cavity.

Cavities have large quality factors, usually several thousands and this means that oscillations of the electromagnetic field fade very slowly. The electromagnetic field induced in the cavity can influence the beam. To decrease the effect of the cavity on the beam its quality factor should be decreased.

Electromagnetic field excited by the beam has an infinite amount of modes with different geometries in the volume of the cavity. The larger the flux into the coupling loop, the larger is its interaction with the magnetic field. Position and size of the coupler which is connected to the external circuit will define which modes of the magnetic field will interact with a coupler. Choosing the position of the coupler will increase influence of the external circuit on the overall loaded quality factor.

Loaded quality factor depends on external quality factor and quality factor Q_0 (see Eq. 1) which is defined only by materials and geometry of the cavity. On the other hand, Q_l is a quality factor of the system when connected to generator and measurement circuits [1]. The relation between them is as follows

$$\frac{1}{Q_l} = \frac{1}{Q_{ext}} + \frac{1}{Q_0} \qquad (1)$$

where Q_{ext} is a quality factor of the external loading circuit. Loaded quality factor can be calculated using frequencies, where the imaginary of the one port scattering parameter is at its maximum and minimum, while phase of the central frequency is normalized [1] (see Eq. 2). This information can be obtained using a vector network analyser.

$$Q_l = \frac{f_{resonant}}{|f(Im(S_{11})_{\max}) - f(Im(S_{11})_{\min})|} \qquad (2)$$

where S_{11} is the reflection S-parameter. In order to check dependency of the loaded quality factor on the external resistivity, several important values of loading were measured.

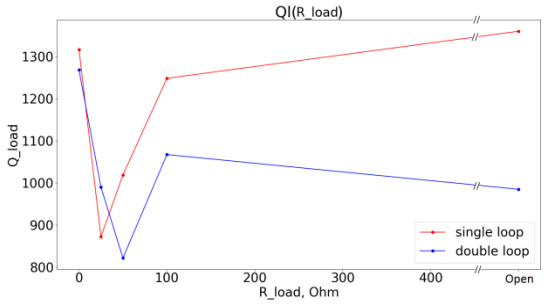

Figure 2: Dependency of the loaded quality factor of the cavity on external resistance for magnetic couplers with single and double loop.

For these measurements different resistances were connected to the single and double loop magnetic couplers. Measurements on a prototype show that mode-dependent loading can decrease loaded quality factor by 30% (Figure 2). Efficiency of this method is limited by the position, orientation and size of the coupler.

It is planned to apply this method in a prototype resonant Schottky cavity [2] in ESR.

References

[1] F. Caspers, “RF engineering basic concepts the Smith chart”, CERN, Geneva, Switzerland, 2010.

[2] S. Sanjari et. al. Current scientific report.

Experiment beamline: ESR
Experiment collaboration: APPA-SPARC / NUSTAR-ILIMA
Accelerator infrastructure: ESR, CR, HESR
PSP codes: 1.2.6.3 and 1.3.1.3.12
Grants: ERC-2015-CoG (ASTRUm - 682841)
Strategic university co-operation with: Heidelberg

Excitation cross sections of hydrogenlike uranium in collisions with hydrogen and nitrogen targets

G. Weber[1], A. Gumberidze[2], A. Surzhykov[3,4], C. J. Fontes[5], and Th. Stöhlker[1,2,6]

[1]Helmholtz Institute Jena, Germany; [2]GSI, Germany; [3]PTB, Germany; [4]TU Braunschweig, Germany; [5]Los Alamos National Laboratory, USA; [6]FSU Jena, Germany;

Electron impact excitation (EIE) and proton impact excitation (PIE) of bound electrons belong to the most fundamental atomic physics interaction processes. Compared to ionization, excitation is mediated by the same interaction mechanism, but the bound electron is excited into a bound state of the ion and not into the continuum. Therefore, the final state of the electron after the collision can be determined by measurements of the deexcitation photons, which allows for a rigorous testing of corresponding theories. While in particular EIE excitation of few electron ions, such as hydrogenlike argon, titanium and iron, has been thoroughly studied in electron beam ions traps [1], for probing of relativistic effects, i. e. the generalized Breit interaction (GBI) [2,3], high-Z ions that are available at GSI provide the best conditions.

Indeed, a recent study of the Lyman radiation emitted by hydrogenlike uranium in collisions with hydrogen and nitrogen gas targets allowed the first identification of the GBI contribution in EIE of a high-Z system [4,5]. The measurement was performed at the internal gas target of the experimental storage ring of GSI, Darmstadt where an array of standard Ge(i) detectors were recording the x-ray emission from the interaction zone of the ion beam and the gas jet target. After capturing a target electron the down-charged projectiles were recorded by a MWPC detector located downstream after the next dipole magnet. Applying a coincidence condition between x-rays and down-charged ions allows identifying those spectral features that are associated with the capture of target electrons into bound projectile states. This is illustrated in Fig. 1 where the photon spectrum coincident with electron capture is contrasted to the one which is not associated to a change of the projectile charge and that contains Lyman emission subsequent to the excitation of the projectile in collisions with target atoms. The previous study of projectile excitation [4,5] concentrated on the intensity ratio of the Ly-a_1 line ($2p_{3/2}$ to $1s_{1/2}$) to the Ly-a_2 ($2s_{1/2}$, $2p_{1/2}$ to $1s_{1/2}$) line that reflects a significant enhancement of the EIE cross section due to the GBI which populates preferentially the j=1/2 orbitals.

In a follow-up study we now aim to determine not only relative excitation cross sections (ground state to the L shell) but absolute ones by normalizing the observed Lyman radiation intensity to the intensity of the radiation emitted in the capture of target electrons into the K and L shell of projectile (K- and L-REC). Since in light targets the electrons are only loosely bound, they can be treated as quasi-free, making REC similar to the radiative recombination (RR), which is the time-inverse of the well-understood photoelectric effect.

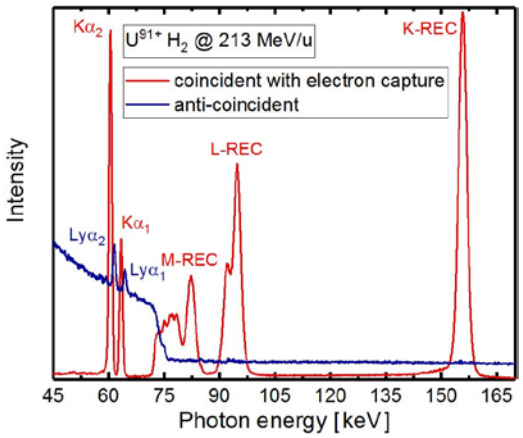

Figure 1: X-ray spectrum recorded by a Ge(i) detector located at 120° with respect to the ion beam axis.

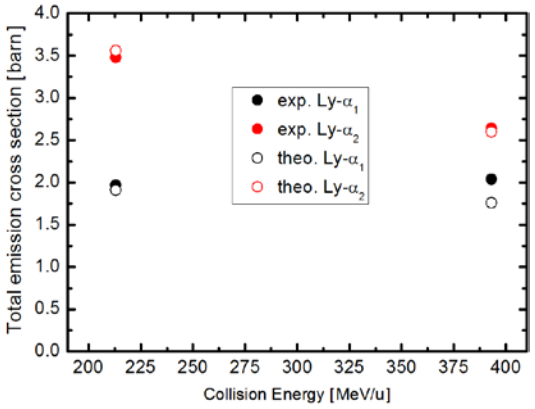

Figure 2: Preliminary results for K-L excitation cross sections for U^{91+} in collision with hydrogen atoms.

Preliminary results of this analysis are shown in Fig. 2 for the collision of hydrogenlike uranium with hydrogen atoms. Theoretical predictions combine both PIE as well as EIE, the latter including the GBI. Note that the population of n=2 states by cascades from higher lying states is not included yet in the theoretical values.

[1] D. L. Robbins et al., Phys. Rev. A 74, 022713 (2006).
[2] C. J. Bostock et al., Phys. Rev. A 80, 052708 (2009).
[3] C. J. Fontes et al., Phys. Rev. A 49, 3704 (1994).
[4] A. Gumberidze et al., Phys. Rev. Lett. 110, 213201 (2013).
[5] A. Gumberidze et al., J. Phys. B 48, 144006 (2015).

Experiment collaboration: APPA-SPARC
Accelerator infrastructure: ESR

 DOI:10.15120/GR-2018-1

A status report on 2D Compton polarimeter development

U. Spillmann[1], T. Krings[2], M. Vockert[3,4], G. Weber[3], and Th. Stöhlker[1,3,4] on behalf of the SPARC collaboration

[1]GSI, Darmstadt, Germany; [2]IKP, FZ-Jülich, Germany; [3]HI Jena, Germany; [4]IOQ, Friedrich Schiller Universität Jena, Germany

For the experimental program of the SPARC collaboration [1] at GSI and FAIR, x-ray spectroscopy and x-ray polarimetry are essential tools.

Polarization of x-rays coming from recombination processes induced by collisions of heavy and highly charged ions at relativistic energies with electrons or low-density gaseous targets provides a unique insight into the dynamics of charged particles in extremely strong and temporally short electromagnetic fields. Detailed knowledge of these processes has, besides atomic physics itself, a great relevance for plasma- and astrophysics.

During the last years we continuously strengthened the instrumentation portfolio of SPARC with dedicated Si(Li)-and Ge(i)-Compton polarimeters which we employed very successfully in experiments at GSI and other research labs, like DESY and ESRF. This technology is based on LN_2-cooled planar double-sided structured detectors (Li-drifted silicon or high purity germanium bulk) with thicknesses in the range of 10 mm. The optimization of such systems for different energy regimes is an ongoing effort.

In this context we designed two test systems where the discrete preamplifier stage was replaced by ASICs to study the pros and cons with focus on a multi-channel readout solution. A 16-pixel HPGe(i) detector was equipped with Cube-ASICs which were run in the transistor-reset as well as in the resistor-reset mode [2]. With this chip we measured the best spectroscopic resolution for our systems up to now. Unfortunately the very high price per channel will only allow for the implementation in very special cases.

In the second study we built a system based on the PIXIE-ASIC[3], developed by Rutherford Appleton Laboratory (RAL), bonded to a linear Si(Li) pixel detector and later to a linear Ge(i) pixel detector. The PIXIE ASIC was developed by RAL to study the properties of CdTl and CdZnTe detectors with small pixel structures at room temperature.

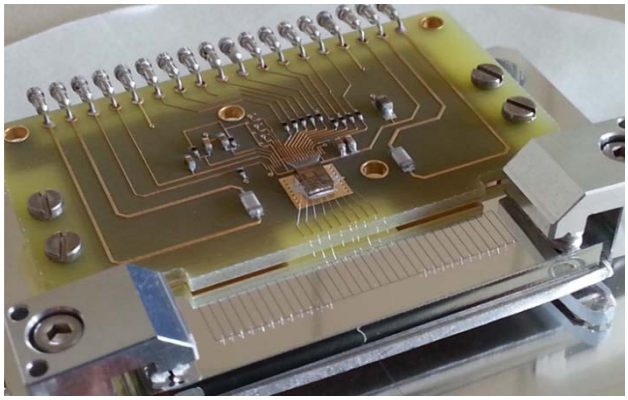

Figure 1: The test pcb with the PIXIE ASIC bonded to a test detector.

Finally we were able to show that this chip, although cooled down to 200 K and operated with higher detector capacitance than allowed by the specs, was able to produce nice results. With pixel structures of 1x5mm^2 we achieved 1.5 keV resolution at 60 keV x-ray energy. This is comparable with discrete preamps run at room temperature. The ASIC pcb is at least by a factor 5 more compact compared to discrete preamps. This test has proven the usability of this technology for a multi-channel readout ASIC for Si(Li)- and Ge(i)-detectors. With minor modifications, to adapt the ASIC especially for these semiconductors, the spectroscopic performance could even be more optimized.

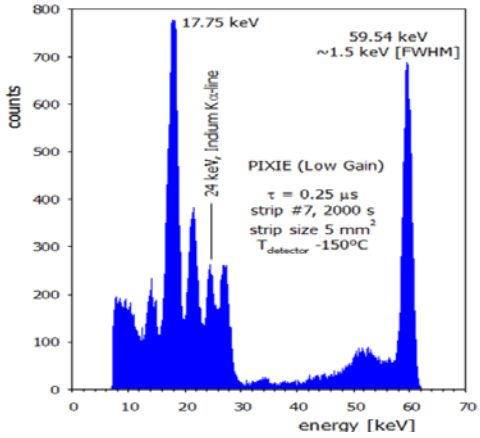

Figure 2: Spectroscopic results of the PIXIE ASICs with Si(Li) pixel detector irradiated with a Am-241 x-ray source.

We like to thank P. Seller, M. French, M.C. Veale, J. Lipp, L.L. Jones, A. Hardie from STFC, RAL(United Kingdom).

This report is also part of the HI Jena Scientific Report 2017.

References

[1] Technical Report of the SPARC collaboration https://www.gsi.de/work/forschung/appamml/atomphysik/ap_und_fair/sparc/dokumente.htm

[2] T. Krings et al., 2015 JINST 10 C02043

[3] M.C. Veale et al., IEEE Trans. Nucl. Sci., vol. 58, no. 5, October 2011, pp. 2357-2362

Experiment beamline: none

Experiment collaboration: APPA-SPARC

Experiment proposal: none

Accelerator infrastructure: none

PSP codes: none

Grants: supported by BMBF Verbundprojekt 05P15SJFAA

Strategic university co-operation with: FSU Jena

Electron capture decay of hydrogen-like ^{142}Pm ions: status of data analysis

F. C. Ozturk[1,2], F. Bosch[1,], P. Bühler[3], R. B. Cakirli[2], T. Faestermann[4], H. Geissel[1], P. Kienle[4,**], C. Kozhuharov[1], Yu. A. Litvinov[1], F. Nolden[1], Y. Oktem[2], N. Winckler[1], M. S. Sanjari[1], C. Scheidenberger[1], M. Steck[1], Th. Stöhlker[1,5,6], and the TBWD Collaboration*

[1]GSI Darmstadt; [2]Istanbul University; [3]SMI Vienna; [4]TU Munich; [5]HI Jena; [6]University Jena

Observation of the modulated behavior of electron capture (EC) decays in hydrogen-like 140Pr and 142Pm [1] caused an extensive controversial discussion in literature which called urgently for a confirmation or disproof of the effect. Therefore, significant efforts have been devoted to the improvement of the non-destructive detection of stored highly-charged ions in the ESR. A resonant cavity-based Schottky detector has been successfully designed, built and installed into the ESR [2]. Owing to the highly increased sensitivity, this novel detector has greatly contributed to numerous nuclear-, atomic- and astrophysics experiments at the ESR [3]. Furthermore, other storage ring facilities are now equipped with such detectors.

However, the largest boost has been given to the Single-Ion Decay Spectroscopy. The experiment mentioned at the beginning has been repeated with hydrogen-like 142Pm ions. Compared to the first experiment, about eight times larger statistics, namely 8665 EC decays, were recorded. The entire set of new decay data did not show any significant modulation [4]. However, one long series of about 4000 consecutive EC decays indicated some oscillatory behavior at the same frequency but with about two times smaller amplitude and a slightly different phase than in the first experiment [4]. A possible explanation could be a failure to remove the “old” ions before the injection of the new ions into the ESR. In such case the start time of the modulation would be smeared out.

A dedicated EMMI Rapid Reaction Task Force took place in July 2014 in Jena. In an open discussion a clear recommendation has been formulated that the experiment has to be repeated under conditions as close to the ones in the first experiment as possible. In the new experiment, which was carried out in fall 2014, more than 10000 EC decays of 142Pm ions have been precisely measured. Attention has been given to the monitoring of all relevant accelerator parameters. Special efforts were made to achieve the reliable emptying of the ESR (from the “old” ions) before every new injection.

The data were analyzed manually and with an automated procedure [5] leading to consistent results. New data can well be described by an exponential decay curve with the decay constant λ=0.0140(6) s-1. No significant modulation is observed. In order to explain the contradiction with the first experiment further studies would be required, probably addressing the hydrogen-like 140Pr ions which have a longer half-life. The corresponding publication is in preparation [6].

* deceased
** deceased

References

[1] Yu. A. Litvinov et al., Phys. Lett. B 664 (2008) 162.
[2] F. Nolden et al., Nucl. Instr. Meth. A 659 (2011) 69.
[3] F. Bosch et al., Prog. Part. Nucl. Phys. 73 (2013) 84.
[4] P. Kienle et al., Phys. Lett. B 726 (2013) 638.
[5] P. Buehler, Nucl. Instr. Meth. A 819 (2016) 167.
[6] F. C. Ozturk et al., Nucl. Phys. A, in preparation (2018).

Experiment beamline: ESR / FRS
Experiment collaboration: APPA-SPARC / NUSTAR-ILIMA / TWBD
Experiment proposal: E077 / E082
Accelerator infrastructure: SIS18 / ESR / FRS
PSP codes: none
Grants:
Scientific Research Project Coordination Unit of Istanbul University. Project numbers: 48110, 54135 and 53864;
European Research Council (ERC) under the European Union's Horizon 2020 research and innovation programme (grant agreement No 682841 "ASTRUm");
Helmholtz Chinese Academy of Sciences Joint Research Group HCJRG-108
Strategic university co-operation with:
Technical University Munich;
JL University Giessen;
RK University Heidelberg;
FS University Jena;
Istanbul University;
North-West Normal University Lanzhou

 DOI:10.15120/GR-2018-1